UNIVERSITY OF CAPE TOWN
IYUNIVESITHI YASEKAPA • UNIVERSITEIT VAN KAAPSTAD

Faculty of Science

Department of Oceanography

Seasonal and interannual variability of surface *chlorophyll-a* and sea surface temperature in the Delagoa Bight, Southern Mozambique

By

Verónica Fernando Dove

Dissertation Presented for the Master of Science Degree in Physical Oceanography

South Africa, December 2015

Seasonal and interannual variability of surface *chlorophyll-a* and sea surface temperature in the Delagoa Bight, Southern Mozambique

By

Verónica Fernando Dove

Supervisors:

Professor Frank Shillington

Department of Oceanography, University of Cape Town (UCT)

Professor Michael J. Roberts

Bayworld Centre for Research and Education Partnership

Oceans and Coasts Research- Dep. of Environment Affairs (MCM)

South Africa, December 2015

Abstract

Multi satellite data for surface *chlorophyll-a (Chl-a),* sea surface temperature (SST), sea surface wind (SSW) and sea level anomalies (SLA) have been obtained and analysed over the Delagoa Bight (24-28^{o}S, 32-36^{o}E), southern Mozambique for the period 2003-2012 at monthly time scales. Both descriptive and quantitative analysis using wavelets have been used to obtain a better understanding of the nature of the interannual, seasonal and intra-seasonal variability of the data. Strong seasonal structure and interannual modulation were observed in the area averaged *Chl-a* concentration and SST. The lowest maximum in monthly *Chl a* was in December (0.127 mg.m^{-3}) and the highest in August (0.541 mg.m^{-3}). The lowest maximum in monthly SST was in August (21.8^{o}C) and the maximum in February (27.9 ^{o}C). The *Chl-a* and SST were strongly anti-correlated and both exhibited a well-defined seasonal cycle, contrasting with the SSW and SLA. The daily observations of temperature at 17 meters depth, from the northern Delagoa Bight at Ponta Zavora (24.48 ^{o}S- 35.24^{o} E) for the period 2006-2011, have confirmed a seasonal signal with amplitude of about 6.5^{o}C. Cool coastal water events were found mostly in summer and spring, with maximum amplitude of 6^{o}C. Further analysis of this daily data did not reveal the timing of such events to be regular.

Declaration

I have originally written the present work, with the full support of my supervisors: Prof. Shillington and Prof. Michael Roberts, at the Department of Oceanography, University of Cape Town (South-Africa). Important contributions on the approach used in this study are clearly acknowledged by referencing it within the text.

Verónica Fernando Dove

Acknowledgements

I express my deep gratitude to my supervisors Prof. Frank Shillington and Prof. Michael Roberts for their patience and continuous support throughout the long period of this MSc. My gratitude is extended to Prof. Chris Reason for all the support in order to be able to conclude the studies.

This research was made possible through the collaborative effort from various institutions and individuals. The financial support was provided by the SIDA/SAREC programme through the Eduardo Mondlane University (UEM) in Mozambique. My special appreciation to Prof. Amália Uamusse, Dean of the Faculty of Sciences at UEM and Dr. Almeida Guissamulo, the coordinator of the programme "The Strengthening of Biological and Oceanographic Research at Department of Biological Sciences".

The *in situ* data was collected under the African Coelacanth Ecosystem Programme (ACEP). I thank Ms. Tammy Morris and Mr. Marcel van der Berg for their assistance during my participation in the ACEP cruises.

I thank everyone at the Department of Oceanography for providing assistance whenever it was needed. Special gratitude to Dr. Charine Collins, Dr. Bjorn Backeberg, Dr. Issufo Halo, Dr. Sergio Malauene, Mrs. Nadia Jabaar and Mrs. Claire Khai.

I am grateful to my family and friends for the unconditional support.

Table of contents

List of Figures

List of Tables

CHAPTER ONE – INTRODUCTION

1.1. Background

The coastal and marine ecosystems are among the most biologically productive areas in the world. They provide advantages such as shoreline protection, water quality maintenance, climate regulation and food security for about one third of the world's population living near the coasts, although these represent only about four percent of Earth's total land area (Brown, 2006). Anthropogenic activities exacerbate natural changes and cause loss of biodiversity, as well as increasing greenhouse gases and rising sea level (Pachauri et al, 2014). Therefore it is advisable to monitor changes in the coastal and marine environment.

One of the essential indicators of change in the coastal and marine environment is phytoplankton, a microscopic flora inhabiting the euphotic zone of the ocean and fresh waters (Yoder and Kennelly, 2006). Phytoplankton plays a critical role in the marine food webs and helps to regulate the global climate (Srokosz, 2000; Platt, 2008). The phytoplankton growth in the upper ocean is determined by the availability of sunlight, nutrients (nitrates, silicates, phosphates and iron) and by the rate of predation by zooplankton (Yoder and Kennelly, 2006).

The biomass of phytoplankton is proportional to the concentration of *chlorophyll-a*, (hereafter *Chl-a*), the main pigment responsible for capturing light for photosynthesis (Yoder and Kennely, 2006). The *Chl-a* concentration at the surface of the ocean can be estimated from space using ocean colour satellite sensors which have the advantage of providing global coverage with higher spatial and temporal resolution than *in situ* observations (Srokosz, 2000; Platt, 2008). The global distribution of surface *Chl-a* concentration, Figure 1.1, from the Moderate Resolution Imaging Spectroradiometer (MODIS) on-board Aqua satellite shows higher values at the continental margins, due to the strong influence of winds and terrestrial runoff, and lower values at the gyres. The *Chl-a* distribution pattern is intrinsically related to the variation of sea surface temperature (hereafter SST) and meteorological conditions (Gregg et al., 2005; Vantrepotte and Mélin, 2009).

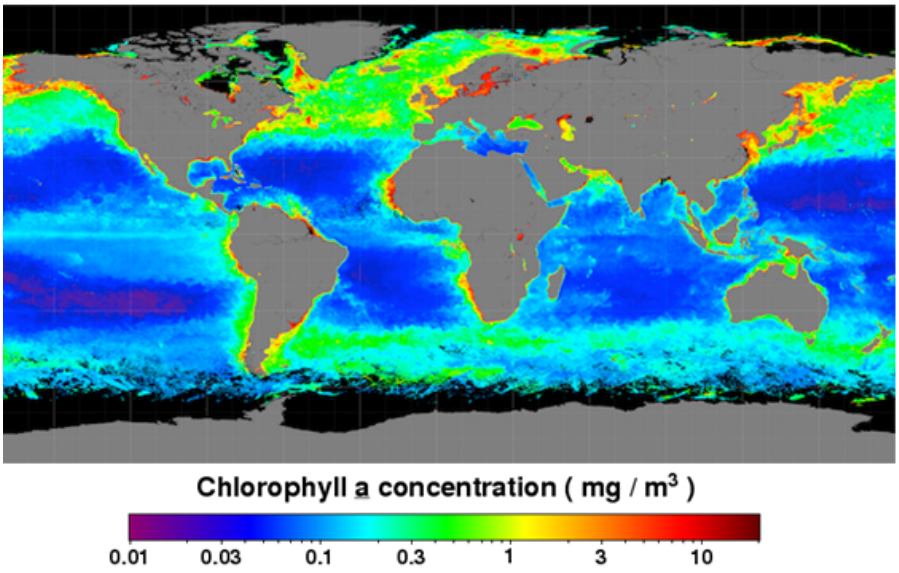

Figure 1.1: Map of annual mean surface Chl-a concentration for 2012 from MODIS Aqua satellite. Higher Chl-a concentration occurs at the continental margins due to higher influence of winds and terrestrial runoff and low Chl-a concentration occurs in the gyres, http://oce ncolor.gsfc.nasa.gov/cgi/l3/.

It has been demonstrated that large scale phenomena such as the El- Niño Southern Oscillation (ENSO) influence the variability of *Chl-a* concentration by changing the wind patterns, the frequency of upwelling events and the dynamics of mesoscale eddies (Murtugudde et al., 1999; Kahru et al., 2010, Curie et al., 2013). Additionally, human activities induce *Chl-a* variability by increasing nutrient inputs, especially in coastal regions. Assessment of the global surface *Chl-a* concentration trends, using satellite ocean colour data, shows discrepant trends. Gregg et al., 2005 using ocean colour reported decreasing trends for most of the open oceans (bottom depth > 200 m) while increasing trends were observed in most of the coastal oceans (bottom depth < 200 m). Wernand et al., 2013 investigated the global *Chl-a* concentration trends using ocean color Forel-Ule scale dataset from 1889 to 2000 and they have shown that the long term trends are highly dependent on the local hydrological and biological conditions. In view of variable trends more research focused on the mesoscale and sub-mesoscale processes for specific regions will contribute to increase the knowledge on *Chl-a* patterns, which is critical for understanding the marine food webs and the global climate (Blondeau- Patissier et al., 2014). In this study we investigate the seasonal and interannual variability of *Chl-a* and its relationship to physical drivers in the Delagoa Bight, southern Mozambique.

1.2. Delagoa Bight

The Delagoa Bight (24-28^{o}S, 32-36^{o}E), located in the southern Mozambique (Figure 1.2) is one of the largest coastline indentations in the eastern coast of Africa (Lutjeharms, 2006, Kyewalyanga et al., 2007; Lamont et al., 2010). The bight plays an important role in the ecology and socio-economics of the South Western Indian Ocean (SWIO). It links the Mozambique Channel flow to the Agulhas Current further south (one of the strongest western boundary currents in the world) (Lutjeharms and Da Silva, 1988; Quartly and Srokosz, 2004). Further, Delagoa Bight is one of the main fishery grounds on the Mozambique Shelf, hosting high biodiversity, including commercial fisheries species such as scad, mackerel and shallow water shrimp (*Penaeus indicus* and *Metapenaeus monoceros)* which yield important food and foreign revenue for the Mozambican economy (Hoguane, 2007).

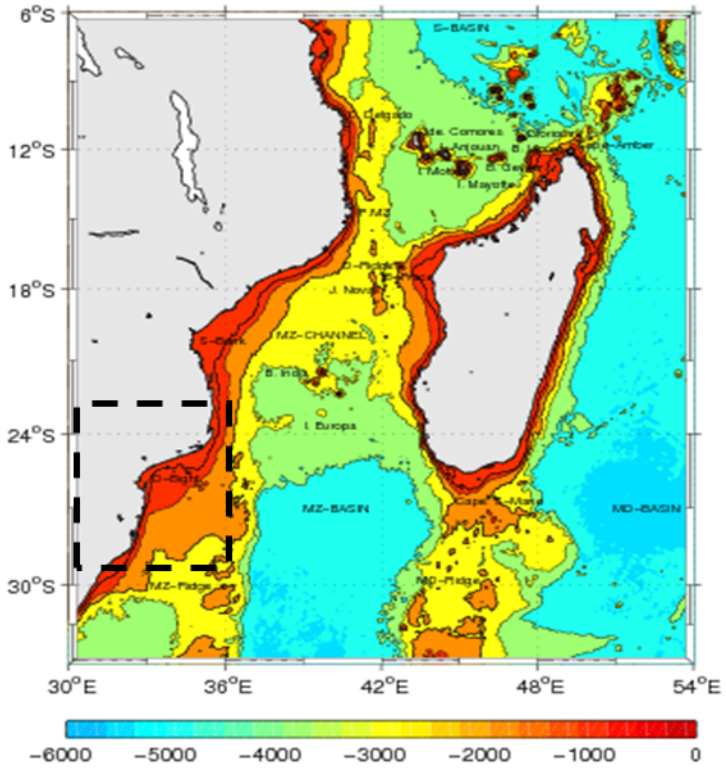

Figure 1. 2: Map showing the Southern Indian Ocean bathymetry. Red areas are the shelf regions with depths less than 1,000 meters. Delagoa Bight is indicated by the black dashed box. (Adapted from Halo, 2012).

The most prominent oceanographic feature in the Delagoa Bight is a cyclonic lee eddy, centred at latitude 26° S and longitude 34° E, with a diameter of ~180 km (Lutjeharms and Da Silva, 1988). The lee eddy in Delagoa Bight is induced by the interaction between the eddies propagating southwards in the Mozambique Channel and the shelf geomorphology (Lutjeharms and Da Silva, 1988; Lutjeharms, 2006). Analysis of sedimentary records suggests the existence of a lee eddy in the Delagoa Bight region for the last 1.8 million years (recent Pleistocene) (Lutjeharms, 2006).

Lutjeharms and Da Silva (1988), using 25 years of *in situ* observations and ten years of satellite sea surface temperature data, investigated the structure and frequency of the lee eddy in Delagoa Bight and concluded that it is a quasi-permanent feature. A different conclusion was drawn by Lamont et al. (2010) who used four sets of hydrographic data, surface drifters and satellite altimetry data to investigate the water masses and circulation in Delagoa Bight. The latter authors suggested that the cyclonic eddy is a transient feature, with its frequency dependent on the movement of eddies in the adjacent waters of Mozambique Channel. The cyclonic lee eddy in Delagoa Bight is well defined below 200 m (Figure 1.3) where it exhibits, in the core of its doming, water temperature and salinity values associated with Antarctic Intermediate Water (AIW) (Lutjeharms and Da Silva, 1988).

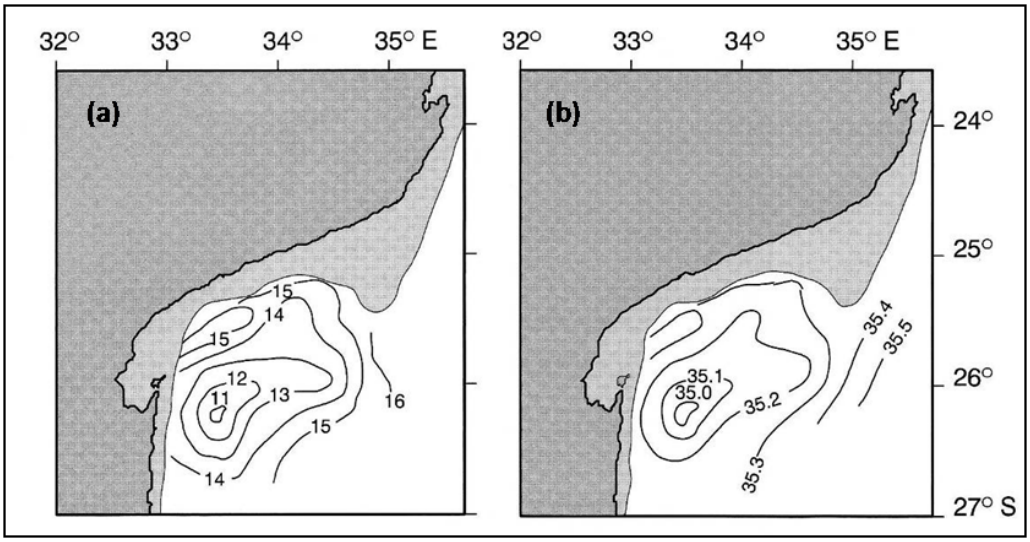

Figure 1.3: Horizontal profiles of (a) temperature and (b) salinity of water upwelled from 900-1000 m in the core of Delagoa Bight cyclonic eddy at 200 m (Lutjeharms and Da Silva, 1988; Lutjeharms, 2006).

Lee eddies are often associated with upwelling structures at the shelf edge which has a persistent western boundary current (Gill and Schumann, 1979; Lutjeharms, 2006). Examples of this along the eastern coast of Africa occur at Natal Bight and Agulhas Bank, where upwelling cells occur at the inshore edges of the Agulhas Current and off southern Madagascar, the latter due to the existence of the East Madagascar Current (Lutjeharms 2006; Lamont et al., 2010). Delagoa Bight has similar coastal geomorphology to the above locations. Although no dedicated literature exists, a well-defined warm western boundary current was observed along the 1,000 m isobaths (Lutjeharms and Da Silva, 1988). IMR (1978) reported a coastal northward current with speeds ranging from ~25.7 to 51.4 cm. s^{-1} during August-October (mid winter to early spring) as estimated from ship drifts, whereas Lamont et al. (2010), using surface drifters, observed a northward current with speeds of ~25–30 cm. s^{-1} during May and August 2004, April 2005 and April 2006.

Delagoa Bight is one of the Mozambican Shelf regions with elevated *Chl-a* concentration (0.6-1.26 $mg.m^{-3}$), often apparent from the ocean colour images as shown in Figure 1.4(a) (Quartly and Srokosz, 2004; Kyewalyanga et al., 2007; Sá et al., 2013). The other two sites with elevated *Chl-a* concentration along the shelf are the Sofala Bank, in the central shelf,

and Angoche in the northern shelf (Lutjeharms 2006; Malauene et al., 2014). The enhanced *Chl-a* in Delagoa Bight is associated with upwelling of cold, nutrient- rich waters on the northern shore, driven by the interaction of the local topography with the mesoscale eddies propagating southwards in the adjacent waters of the Mozambique Channel (Lutjeharms and Da Silva, 1988; Quartly and Srokosz, 2004; Lutjeharms, 2006; Barlow et al., 2008; Roberts et al., 2014).

M. Roberts (pers. Comm., 2008) schematized the main oceanographic features for Delagoa Bight (Figure 1.4b) based on the existing regional oceanographic studies e.g. for the Agulhas Current System and Mozambique Channel (Lutjeharms and Da Silva, 1988; Quartly and Srokosz, 2004; Lutjeharms, 2006; Barlow et al., 2008). The oceanographic features in the Delagoa Bight include (i) a coastal *Chl-a* concentration ribbon in the northern shore, (ii) the Ponta Zavora *Chl-a* concentration plume and (iii) the cyclonic flow.

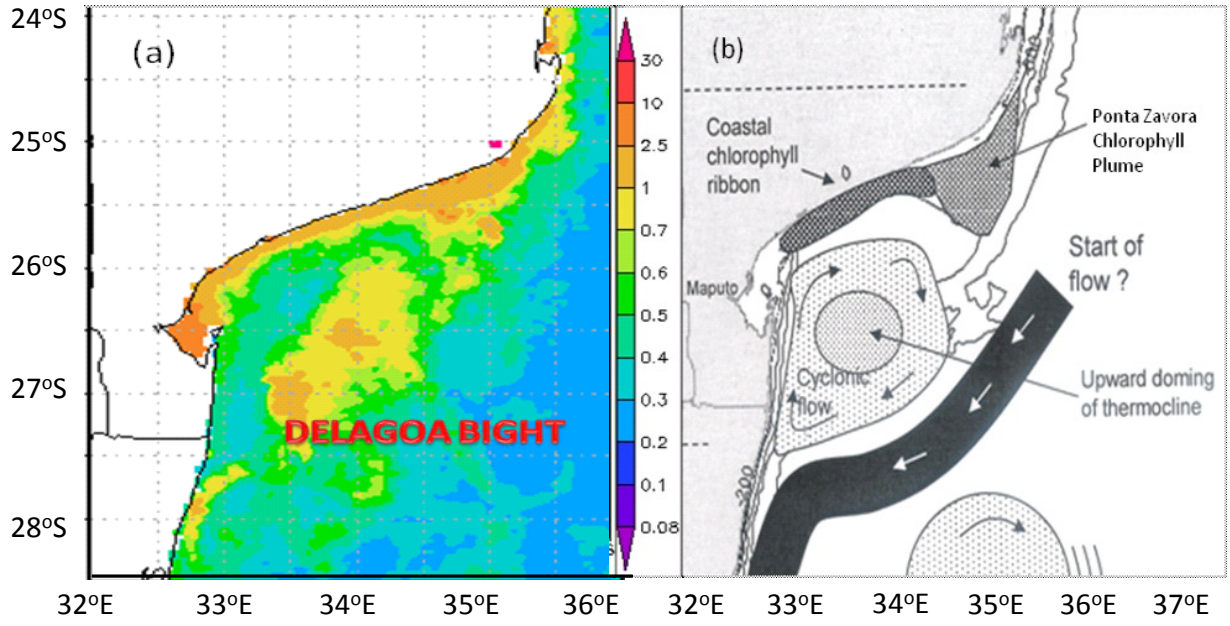

Figure 1.4: (a) MODIS Aqua image of monthly Chl-a concentration for August 2003 in Delagoa Bight (http://giovanni.gsfc.nasa.gov), (b) schematic of the main oceanographic features in Delagoa Bight (Michael Roberts, pers. comm., 2008).

M. Roberts (pers. comm., 2008) hypothesised that the coastal *Chl-a* concentration ribbon and the Ponta Zavora *Chl-a* concentration plume are a biological response to the Limpopo

River leaching and the upwelling cell in the northern Delagoa Bight. It has been demonstrated that mesoscale eddies through the eddy pumping, can uplift the nutricline, thus enhancing primary production (McGillicuddy et al., 1998). To date, the temporal and spatial variability of the phytoplankton productivity associated with the cyclonic flow in the Delagoa Bight has not been assessed.

1.3. Motivation for the study

The majority of the existing research on the phytoplankton abundance (*Chl-a* concentration) and its relationship with the physical drivers for Delagoa Bight region results, mainly, from the use of short term datasets (*in-situ* and satellite) and research designed for larger domains e.g. the Agulhas Current System and the Mozambique Channel (Lutjeharms and Da Silva, 1988; Quartly and Srokosz, 2004; Barlow et al., 2008; Lamont et al., 2010, Sa et al., 2013; Roberts et al., 2014). Further, the studies of water temperature in Delagoa Bight have been conducted using short term measurement instruments (e.g. conductivity, temperature and depth profiler, CTD and the expendable bathythermography, XBT) and infrared data (Lutjeharms and Da Silva, 1988; Lamont et al., 2010). Factors limiting the studies on the *Chl-a* concentration and water temperature studies in Delagoa Bight include the low coverage of cruise data.

The availability of (i) *in situ* water temperature dataset collected under the framework of the African Coelacanth Programme (ACEP) during 2006- 2011, and (ii) satellite datasets from MODIS Aqua and TOPEX/POISEDON which have high spatial and temporal resolution at the mesoscale (~10– 50 km, monthly sampling) provided the initial motivation to carry out this study. Further motivation was gained by undertaking an exploratory approach where a total of 456 weekly *Chl-a* composites, from MODIS Aqua (4 km resolution) for 2003-2012, were visually inspected using the GES-DISC Interactive Online Visualization and Analysis Infrastructure (GIOVANNI) animation mode, http://gdata1.sci.gsfc.nasa.gov/daac-bin/G3/gui.cgi?instance_id=ocean_8day/.

The visual inspection showed *Chl-a* concentration patterns consistent with the features schematized by M. Roberts (pers. comm., 2008), although in many occasions they were

partially or totally obscured by clouds. Figure 1.5 shows chosen images for illustrative purposes where the features are fully developed.

A study of the *Chl-a* concentration variability and the physical drivers using both long term satellite and *in situ* data sets will contribute to improve the understanding of the Delagoa Bight ecosystem functioning. In this study we aim to provide the seasonal and inter-annual variability of *Chl-a* concentration, its relationship with sea surface temperature (SST), sea surface winds (SSW) and sea level anomalies (SLA) for 2003-2012. Further, we seek to assess the frequency and duration of upwelling events in the northern Delagoa Bight using a 5-year *in situ* water temperature dataset collected during the ACEP. This thesis concentrates mainly on an understanding of the seasonal and interannual variability using monthly data. Weekly images were used in an exploratory assessment of the *Chl-a* variability (Figure 1.5). These images hint that the short term variability will exceed the seasonal variability. This aspect has not been the main focus of the thesis.

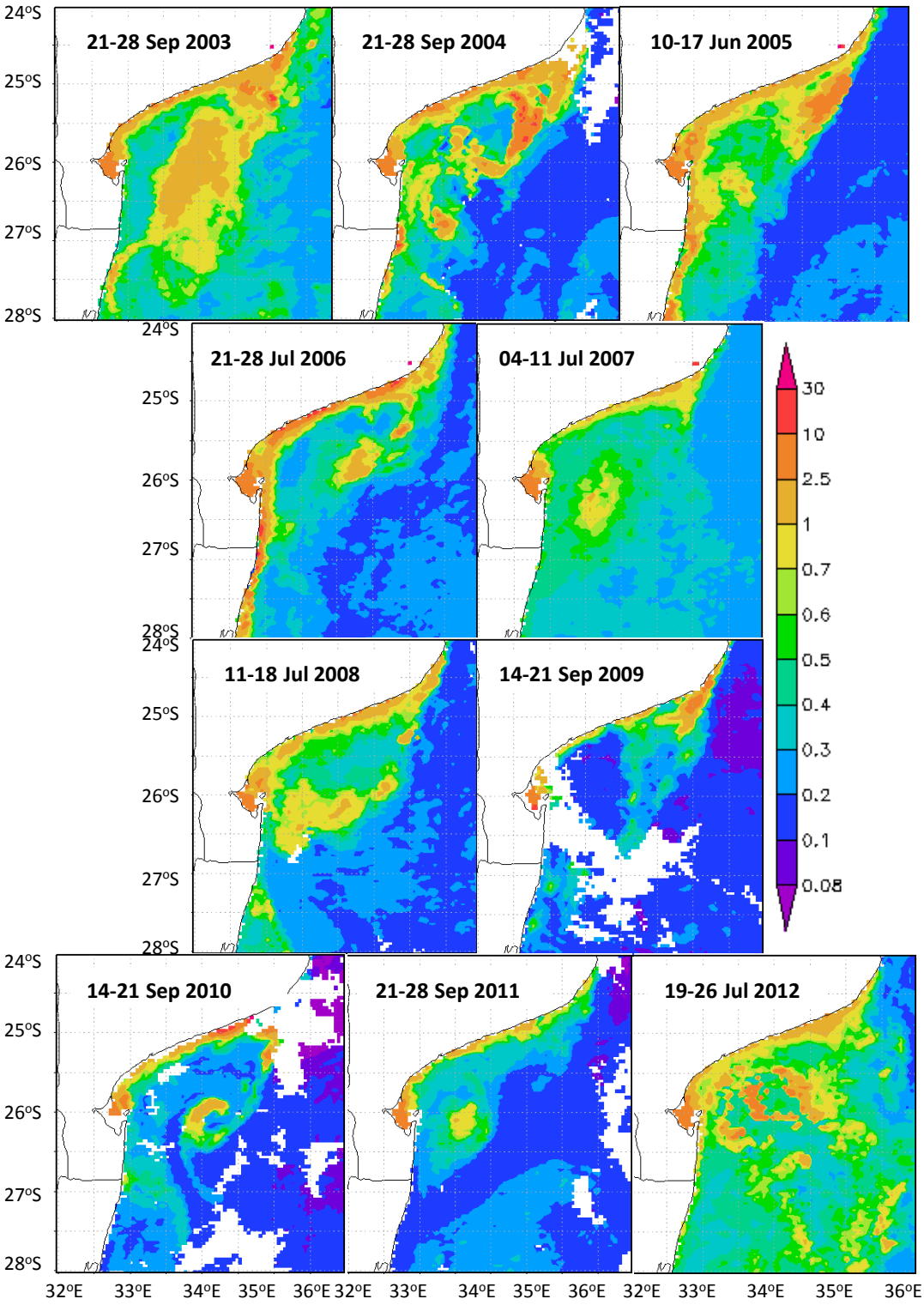

Figure 1.5: Weekly composites of MODIS Aqua Chl-a concentration (4 km resolution) for Delagoa Bight showing consistent patterns with the oceanographic features schematized by M. Roberts (pers. comm., 2008).

1.4. Research objectives

The main objective of this dissertation is to investigate the seasonal and interannual variability of *Chl-a* concentration in Delagoa Bight and to understand its relationship with the water temperature, sea surface winds and sea level anomalies during 2003-2012. Further, the frequency and duration of cool water events for the northern Delagoa Bight will be assessed. Our goal is to quantify and compare biological and physical variability in the Delagoa Bight (Figure 4.1). The information on this variability will contribute to improve the knowledge on the Delagoa Bight ecosystem functioning. Delagoa Bight plays an important role in the flow, ecology and biodiversity of the inshore region of the Agulhas current (Lutjeharms and Da Silva, 1988) and in the Mozambique Channel and Shelf (Hoguane, 2007; Lutjeharms 2006). The results from this study are relevant for fisheries and climate research in the adjacent countries of the SWIO.

1.5. Research questions

- What is the seasonal and interannual variability of surface *Chl-a* concentration at Delagoa Bight in relation to sea surface temperature, sea surface wind and sea level anomalies?
- What is the frequency and duration of cool water events in the northern Delagoa Bight?

1.6. Outline of the dissertation

The dissertation contains six chapters. The Introduction presents the background, the relevance of the study and the objectives. Chapter Two presents the literature review on the Mozambique Channel, Mozambican Shelf mesoscale processes and their influence on the *Chl-a* concentration (phytoplankton) and the conceptual aspects of remote sensing of ocean colour and radiometry. Chapter Three describe the *in situ* and satellite data sets and methodologies used to process the data. Chapter Four presents the results. Chapter Five presents the Discussion. Chapter Six summarises the main conclusions and provides some recommendations for a continuation of the present work in the future.

CHAPTER TWO - LITERATURE REVIEW

2.1. Phytoplankton and environmental conditions

2.1.1. Phytoplankton and primary production

Phytoplankton are microscopic free-floating unicellular organisms inhabiting the euphotic zone of the ocean and fresh waters typically within the upper 50-100 m of the water column (Lalli and Parsons, 1997). About 5000 species of marine phytoplankton have been studied worldwide and their size range from less than 1 μm to over 100 μm (Blondeau-Patissier et al., 2014). The most studied groups of phytoplankton are diatoms, dinoflagellates and coccolithophorids (Lalli and Parsons, 1997). The diatoms are the dominant type from the temperate and high latitudes regions. Due to their nature, diatoms are negatively buoyant with a tendency to sink rapidly out of the surface layer of the ocean contributing to the transport of carbon, nitrogen and silica to deeper waters (Lalli and Parsons, 1997). Dinoflagellates are the second dominant phytoplankton type at the sea and they have the ability to move in the water. Coccolithophorids are generally smaller than 20 μm.

Phytoplankton constitute the major primary producers which use the solar radiation to convert inorganic material into new organic compounds through the photosynthesis process, therefore starting the marine food webs (Lalli and Parsons, 1997: Helbling and Villafane, 2007). The plant tissue produced over the time during the photosynthesis is the primary production (Lalli and Parsosn, 1997). Although phytoplankton organisms constitute only 1-2% of the total global biomass they play an important role for being responsible for fixing ~30-60% of the global annual fixation of Carbon Helbling and Villafane, 2007). Additionally phytoplankton contributes for the biological pump (Figure 2.1), the collectively processes involving the transport of inorganic carbon from the sea surface to greater depths thus contributing to reduce the global warming (Ducklow and Buesseler, 2001). The thermohaline circulation is responsible for returning deep-ocean dissolved inorganic carbon to the atmosphere on millennial timescales.

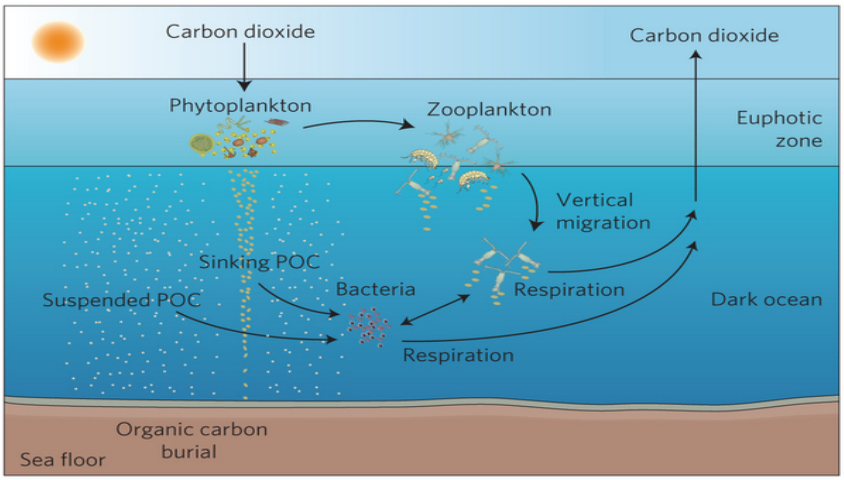

Figure 2.1: Biological pump diagram. The pelagic environment in the coastal and open-ocean waters is generally comprised by algal groups adapted to the environmental conditions (Adapted from Ducklow and Buesseler, 2001).

2.1.2. Oceanic processes in relation to phytoplankton growth

The phytoplankton biomass growth in the upper ocean is determined by the availability of sunlight, nutrients (nitrate, silicate, phosphate and iron) and by the rate of predation by zooplankton (Yoder and Kennelly, 2006). The change in the phytoplankton population dynamics occurs as response to physical driving mechanisms, which have different time scales. These mechanisms include the terrigenious runoff, winds, upwelling and mesoscale eddies (Cloern, 1996). In response to these mechanisms many species of phytoplankton may have a rapid cell division and population growth with a possible formation of phytoplankton blooms, defined as a deviation (increase) from a baseline biomass (Lalli and Parsons, 1997, Cloern, 1996).

The phytoplankton blooms can be quantified by the use of *Chl-a* concentration, parameter used to establish the standards for a bloom in a specific system but due to differences in the trophic levels these standards can hardly be extrapolated from a system to another. Table 2.1 shows the throphic level classification according to the *Chl-a* concentration in a water body (Shushkina et al., 1997 quoted by Kletou and Hall-Spencer, 2012).

Table 2. 1: Thophic level classification for water bodies according to *Chl-a* concentration according to Shushkina et al., 1997 quoted by Kletou and Hall-Spencer, 2012)

Water body class	*Chla* (mg.m -3)
Ultraoligotrophic	<0.06
oligotrophic	0.06-0.1
Mesotrophic	0.1-0.3
Eutrophic	0.3-1
Hypertrophic	>1.00

Due to the different time scales variability of the physical mechanisms driving the phytoplankton blooms they can, generally, be classified into three main types: (i) aperiodic events that often last for days (ii) recurrent seasonal events which last for weeks and (iii) exceptional events typically dominated by few species which last for months (Cloern, 1996).

2.2. Solar radiation in the ocean

Solar radiation drives all the biological and physical processes on the Earth. The amount of light reaching the surface of the ocean varies with the time of the day, the season and the weather (Lalli and Parsosns, 1997). The electromagnetic spectrum wavelengths are shown in Figure 2.2. About 50% of the solar radiation penetrating the sea has the wavelengths is within the visible spectrum of ~ 400-700 nm (known as light and to which human eye is sensitive and correspond to the photosynthetically active or available radiation (PAR), the light interval used by plants (including phytoplankton) for photosynthesis (Srokosz, 2000; Lalli and Parsosns, 1997).

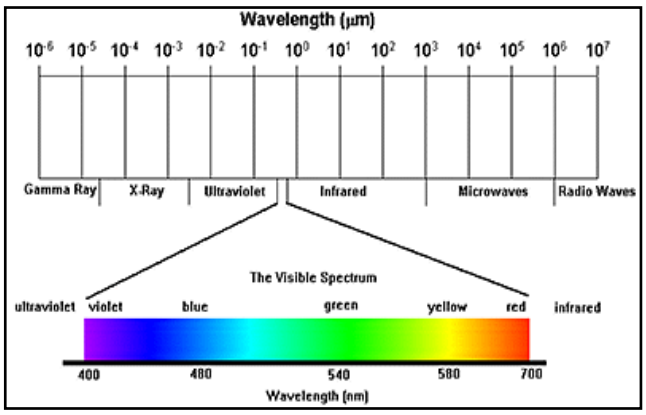

Figure 2.2: Electromagnetic spectrum from Radio waves to Gamma rays with the visible part expanded (http://www.crisp.nus.edu.sg/~research/tutorial/em.htm/).

Water absorbs warm long wavelength light (e.g red and orange) and scatters short wavelength light. Phytoplankton contains *Chl-a* and this pigment absorbs light at blue (450 nm) and red (650 nm) wavelengths and transmits in the green (520 nm). The *Chl-a* property of absorbing light can used to estimate the phytoplankton (*Chl-a*) in the coastal and ocean waters from space.

2.3. Optical properties of natural waters

According to their optical properties, natural waters can be classified into Case 1 waters (oceanic and less productive waters), mainly influenced by phytoplankton and their co-varying detrital products, and Case 2 waters (coastal and more productive waters), mainly influenced by suspended sediments, dissolved organic matter, *coccolithophore*s, detritus, bacteria and terrigenous particles from rivers (Morel and Prieur, 1977). The optical classification of natural waters is mainly used for ocean colour remote sensing (Srokosz, 2000).

The light (photons) entering the ocean is subject to two physical processes: the scattering and the absorption which are described by the use of two properties: the inherent optical properties (IOPs) and the apparent optical properties (AOPs) (Srokosz, 2000). The main IOPs are the volume scattering function (related to the direction of scattering) and the coefficients of absorption and scattering of light in the medium. The AOPs depend on both the IOPs and the geometric characteristics of the light. Examples of AOPS are the attenuation coefficients which describe the light decrease as the water column increases.

Both IOPs and AOPs depend on the water itself and its constituents such as the phytoplankton (Srokosz, 2000). Figure 2.3 illustrates the penetration of light in the water column for Case 1 and Case 2 waters.

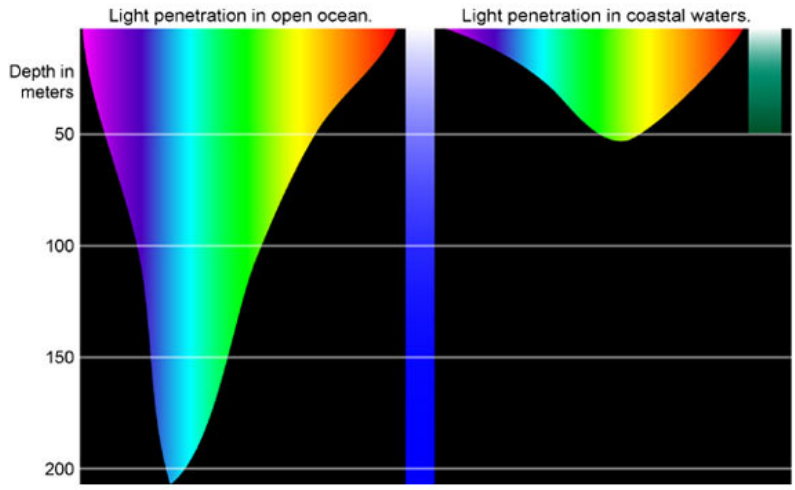

Figure 2.3: Illustration of the penetration of light in the oceanic (Case 1) and coastal (Case 2) waters, where warm colours known as long wavelength light (e.g. red and orange) are absorbed and cooler colours known as short wavelength light (e.g. blue).

2.4. Satellite remote sensing of ocean colour

Remote sensing is a technique used for acquiring information about an object without getting into contact with it. The technique is based on the use of electromagnetic radiation reflected or emitted from the object. Remote sensing is an important tool for mapping the oceanic properties on a very large scale. This tool is fundamental for understanding of the marine processes, ecology and the ocean environmental changes. Due to the atmospheric interaction with electromagnetic radiation (such as absorption and scattering), the ocean can be remotely sensed in three regions of the electromagnetic wavelength bands (atmospheric windows) which are the visible, infrared and microwave.

The colour of a particular water body depends on the interaction between the incident sunlight and the water constituents. Water with low concentration of phytoplankton reflects more blue wavelengths whereas water with high concentration reflects more the green wavelengths (Srokosz, 2000). By using the light spectrum measured by the satellite ocean colour sensor, makes it possible to estimate the *Chl-a* concentration and

consequently the phytoplankton concentration which gives an indicator of the oceanic primary production (Srokosz, 2000). The interpretation of satellite derived *Chl-a,* especially from coastal waters (Case 2 waters) requires cautious analysis due to proximity of land. Suspended sediments, dissolved and particulate organic matter from river leaching can contaminate the satellite signal (Yoder and Kennelly, 2006).

2.5. Satellite remote sensing and radiometry

The sea surface temperature, SST, detection from space is based on the measurement of the surface brightness (radiative intensity) in microwave wavelengths which can be converted to temperature. The High Resolution Sea Surface temperature Pilot Project (GHRSST-PP) (http://ghrsst-pp.metoffice.com/pages/sst_definitions) provides the definition of the SST concepts for the top 10 m of the ocean which are applied for the majority of infrared satellite and ship mounted radiometer measurements (Figure 2.4).

The interface SST is a theoretical temperature at the air-sea interface and it has no practical use as it cannot be measured using current technology. The skin SST is the temperature of the water in a depth of ~20 μm which is potentially affected by factors such as the diurnal cycle and the cool skin layer. The sub-skin SST is the temperature of a layer ~1mm thick at the surface of the ocean. The depth SST also known as SST or "bulk" SST is the in *situ* measurement near the surface of the ocean. The foundation SST product provides an SST that is free of daytime warming or nocturnal cooling. The depth and conditions in which the depth SST is measured has to be always indicated so that it can be applicable for comparison or validation of satellite-derived estimates of SST using other data sources. The Foundation SST is the temperature of the water column free of diurnal temperature variability and it is similar to the night minimum temperature at the depths of ~1-5 m (http://ghrsst-pp.metoffice.com/pages/sst_definitions/).

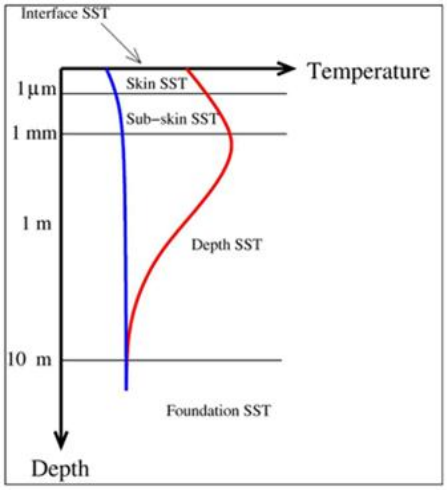

Figure 2.4: Sea surface temperature types as defined by the GHRSST-PP showing examples of night time temperature profiles for the top 10 m of the ocean in conditions of high wind (blue line) and low wind (red line) (http://ghrsst-pp.metoffice.com/pages/.

Besides the satellite platforms measuring only the sea surface temperature, semi-permanent moored instruments such as underwater temperature recorders which allow for collection of long term water temperature data, crucial in the investigation the vertical profiles and upwelling events. Moored buoys or towers equipped with optical and electrical sensors (time-series stations) can measure detailed temporal variations at fixed locations for longer time periods. Water temperature data have large applications e.g. for studies of heat, momentum and moisture gases and characterization of the ocean structures such as fronts, eddies and upwelling.

2.6. Oceanography of Mozambique Channel and Mozambique Shelf

2.6.1. Oceanography of Mozambique Channel

The Mozambique Channel, lying between the southeast African coastline and Madagascar Island, latitudes 10° 20'S-26° 50'S is ~3000 m deep (Kai and Marsac, 2010; Halo, 2012) (Figure 2.1). The channel is an important part of the greater Agulhas Current system, the latter playing an important role for the global ocean conveyer belt (Schouten et al., 2002b; De Ruijter et al., 2006; van der Werf, 2010).

The flow and water masses of Mozambique Channel have been investigated using a combination of hydrographic measurements, satellite data and numerical ocean models. The volume transport varies according to the region of the channel. Using the simplified

Sverdrup model Godfrey (1989) estimated the volume transport to vary from 10-15 Sv, ($1Sv = 10^6\ m^3\ s^{-1}$). Using hydrographic data DiMarco (2002) found 5 Sv and 25 Sv for the northern and the southern channel respectively. In the same location (the southern channel), De Ruijter (2003) found a volume of 14 Sv while Harlander et al., (2009) found 8.6 Sv.

The structure of the main flow, initially considered as a steady continuous Mozambique Current has been investigated by several authors who found discrepancies in the volume flux results (Lutjeharms, 2006) but concordant on its poleward direction (De Ruijter et al., 2002). Ridderinkhof and De Ruijter (2003) using data from current meters deployed across the narrowest part of Mozambique Channel (16^oS) demonstrated that there is no continuous Mozambique Current, instead the main flow is characterized by a train of anticylonic eddies moving southwards.

The anticyclonic eddies are influenced by Rossby waves occur in a frequency of 5-6 per year, with spatial scales of 300-350 km and moving at 6 km/day, in the northern channel, and 3-4 km/day, in the southern channel (Schouten et al., 2003). Halo et al. (2012) used satellite altimetry, transport estimates from *in situ* measurements and outputs from two ocean circulation models, the Hybrid Circulation Ocean Model (HYCOM) and the South-West Indian Model (SWIM), to investigate the mesoscale eddy properties and transport variability in Mozambique Channel. The authors pointed out that during the cyclonic and anticyclonic eddies propagation towards the south, their size is reduced. According to Halo (2012) in the Mozambique channel, cyclonic eddies are in higher number than the anticyclonic, though the flow is dominated by the anticyclonic eddies due to their larger size, higher energy and longer life-time than the cyclonic eddies (Table 2.2).

Table 2. 2: Physical characteristics of the eddies in the Mozambique Channel as from altimetry and the South- West Indian Model (SWIM). Adapted from Halo (2012).

Source of data	Type of eddy	Mean diameter	Mean amplitude	Mean life-time	Annual frequency
Altimetry	Cyclonic	139 km	11 cm	94 days	19
	Anticyclonic	155 km	13 cm	100 days	18
SWIM	Cyclonic	135 km	08 cm	58 days	17
	Anticyclonic	198 km	25 cm	109 days	13

The impact of the mesoscale eddies phytoplankton biomass in the Mozambique Channel and shelf have been studied by several authors. Kai and Marsac (2010) investigating the influence of mesoscale eddies on spatial structuring of top predators' communities in the Mozambique Channel concluded that the edge of eddies provide good foraging conditions for the top predators (frigatebirds and tuna). Roberts et al. (2014) and Barlow et al. (2013) using altimetry and *insitu* data investigated the interaction between eddies in the channel and the continental slope have demonstrated the role of the mesoscale eddies the in the phytoplankton biomass. The authors pointed out that nutrient pumping in the surface waters of the western channel is influenced by the southward movement of eddy dipoles, the same mechanism promoting the exchange of nutrients between the shelf and the open ocean.

Jose et al. (2013) using coupled models**,** the Pelagic Interaction Scheme for Carbon and Ecosystem Studies (PISCES) and the Regional Oceanic Model (ROMS), simulated the impact of mesoscale activity on phytoplankton and nutrient distribution in the Mozambique Channel. They found that phytoplankton growth within the eddies is dependent upon the nutrient advection into the euphotic zone. Huggett (2014) using cruise data investigated the impact of mesoscale features (cyclonic and anticyclonic) in the zooplankton community of the Mozambique Channel and found that the interaction between the eddies and the shelf plays a major role in the pelagic ecosystem by enhancing the growth and redistribution of zooplankton communities.

2.6.2. Oceanography of Mozambique Shelf

The Mozambique shelf width (Figure 2.5) varies from ~100 m, at the narrowest part off Pemba in northern shelf to 145 km in the widest part on the Sofala Bank, central shelf, with an average of ~20 km (De Sousa, 2011). The most thorough investigation on the oceanography off Mozambique coastal waters was conducted by Saetre and Da Silva (1982) to map the water masses and general flow using historical cruise data collected from 1977 to 1980. They identified three large anticyclonic eddies (I, II and III) and four small cyclonic eddies (a, b, c, d) with varying positions and intensities along the year (Figure 2.5). According to these authors the cyclonic eddies were more intense during the southern summer and had a stronger baroclinic structure at ~200 m depth, although they could be detected below 500 m depth.

The mechanisms of formation of the eddies and their ecological impacts on the shelf are diverse. The eddy (a) off Angoche (Figure 2.5) in the northern shelf, is a topographically induced feature (Saetre and Da Silva, 1982) associated with upwelling events, driven by an alongshore north-easterly wind, resulting in enhanced *Chl-a* concentration in an area of ~ 68, 000 km^2 (Malauene et al., 2014). The eddy (b) near Sofala Bank, in the central shelf, is driven by the Zambezi River runoff. The eddies (c) and (e), off Bazaruto and Ponta Zavora respectively, are transient features whereas the eddy (d), at Delagoa Bight, is induced by the topography (Saetre and Da Silva, 1982; Lutjeharms, 1988). Intermittent tropical cyclones bring event-scale rainfall episodes that may totally dominate the annual rainfall distribution.

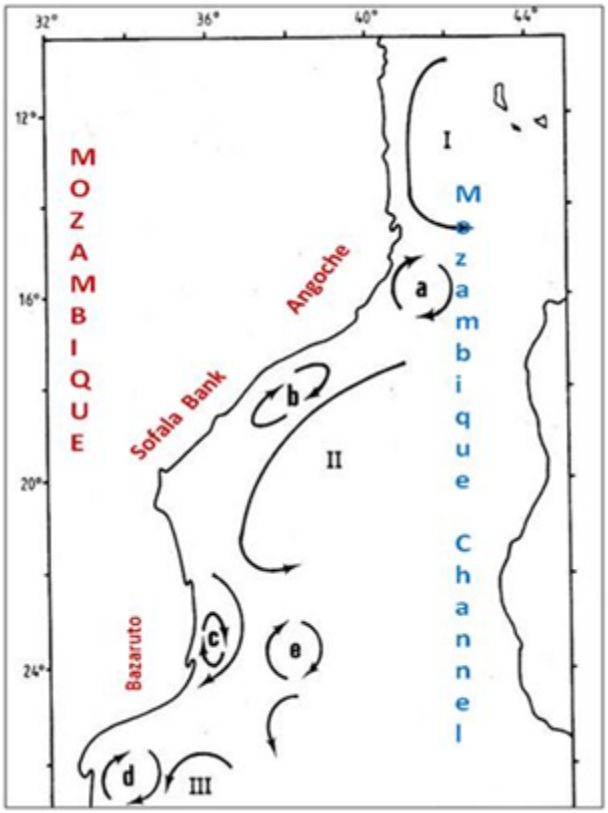

Figure 2.5: Schematic diagram of the main circulation features off Mozambique coast showing large anticyclonic eddies (I, II, III in the northern, central and southern Mozambique respectively) and small cyclonic eddies (a) off Angoche, (b) Sofala Bank (c) and (e) Bazaruto and Ponta Zavora and (d) Delagoa Bight (Saetre and Da Silva, 1982).

CHAPTER THREE - MATERIALS AND METHODS

In this chapter we describe the study area, the *in-situ* and remote sensing data sets and the methodology used in this research.

3.1. Study area

The Delagoa Bight is located in the south-western Mozambique Channel and connected to Maputo Bay from the south-western side. The study domain, 24-28°S, 32-36°E (~4°x4°), is delimited by the red box in Figure 3.1. The main river runoff in the study area is from the Limpopo River. Additional runoff may come through Maputo Bay, which has an area of ~1,000 km^2 and receives drainage from three main rivers namely Maputo, Incomati and Umbeluzi.

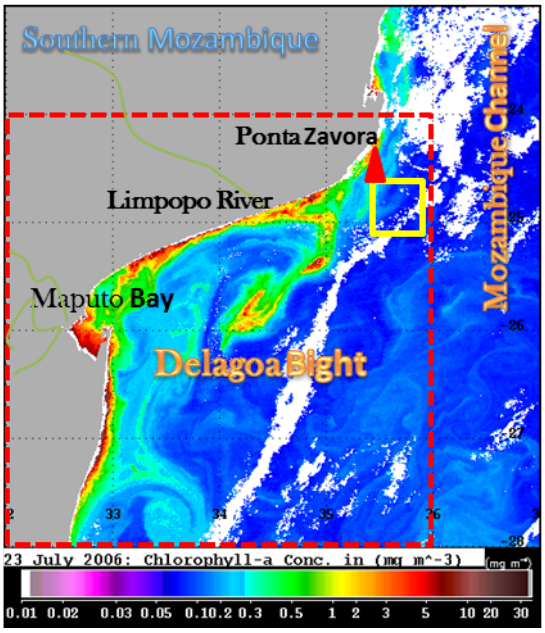

Figure 3.1: Schematic diagram of the main circulation features off Mozambique coast showing large anticyclonic eddies (I, II, III in the northern, central and southern Mozambique respectively) and small cyclonic eddies (a) off Angoche, (b) Sofala Bank (c) and (e) Bazaruto and Ponta Zavora and (d) Delagoa Bight (Saetre and Da Silva, 1982).

Over the study domain (Figure 3.1) we evaluated 10-years (January 2003 to December 2012) of satellite-derived *Chl-a*, SST SSW and SLA data, and 5-years of *in situ* water temperature for the period 23 April 2006 to 22 May 2011. The study domain (24-28°S, 32-36°E) for the extraction of the satellite time series (see section 3.2) was slightly

expanded to 22-28°S, 32-38°E, for the extraction of the horizontal maps in order to better visualize the variable features. The primary variable for this study is the *Chl-a* concentration.

3.2. *In situ* water temperature and data and processing

A 5-year time series of in situ water temperature data recorded by a mini Underwater Temperature Recorder (UTR) during the African Coelacanth Ecosystem programme was used in the study. The UTR was deployed at 17 m depth in the northern Delagoa Bight at Ponta Zavora (24.48°S and 35.48°E), shown by the red triangle in Figure 3.1. The self-contained Star-Oddi UTR which has an accuracy of ±0.05°C was set to record the water temperature at hourly intervals from 23 April 2006 to 22 May 2011. The data, available at http://www.oceanafrica.com, was used to assess the frequency and duration of cool water events in the northern shore of Delagoa Bight. Cool water events were defined as a decrease of ~2°C in the water temperature after Malauene et al. (2014). The hourly data was averaged into daily means by averaging all the hourly (24 records) and the seven days records respectively. Wavelet analysis was applied to the daily anomalies time series with the aim of identifying the main periodicities in the water temperature

3.3. Satellite data sets

3.3.1. Surface *Chl-a,* SST and data processing

The *Chl-a* concentration and SST data used in this study are from the Moderate Resolution Imaging Spectroradiometer (MODIS), a key instrument on-board the Terra (from 1999) and Aqua (from 2002) satellites. MODIS Aqua's orbit around the Earth is timed to pass south to north over the Equator in the afternoon. The satellite views the entire Earth's surface every 1 to 2 days, detecting emitted and reflected radiance in 36 channels spanning the visible to infrared (IR) spectrum, (http://modis.gsfc.nasa.gov/about/specifications.php) MODIS Aqua provides an opportunity to study physical and bio-chemical processes occurring near the sea surface, by providing simultaneous views of both SST and ocean colour (http://oceancolour.gsfc.nasa.gov/).

The details on the MODIS Aqua data processing and distribution are provided in http://oceancolor.gsfc.nasa.gov/DOCS/MODISA_processing.html. There are three levels of MODIS imagery products: L1 are raw radiance measurements recorded at 250m spatial resolution for bands 1 and 2; 500m spatial resolution for bands 3 to 7 and 1 km for bands from 8 to 36. The Level 1A products are radiances without geographic referencing whereas Level 1B products have geographic referencing. The Level 2 products are the derived variables such as SST and *Chl-a* at 1 km spatial resolution covering the same area as the original scene. A Level 3 product is a composite produced by averaging multiple Level 2 scenes over a period (e.g 8 days or a month), with spatial resolution of 4 km or 9 km. MODIS aqua has also Level 3 monthly climatology products resulting from averaging multiple images from the same month over several years.

In this study we used MODIS Aqua Level 3 products at 4 km spatial resolution of the *Chl-a* (weekly and monthly) and the monthly day time SST (11μm). These data are used to investigate the *Chl-a* and the SST variability in Delagoa Bight. The Sea surface temperature data is acquired by satellite remote sensing using microwave (infrared) wavelengths.

The standard bio-optical algorithm for MODIS *Chl-a* is OC3 which uses one of two remote sensing reflectance: Rrs (443/551)/Rrs(488/551) ratios to estimate *Chl-a* from a cubic polynomial formulation, depending on the reflectance characteristics of the water type (O'Reilly et al., 2000). In a 24-hour period, over most of the Earth's ocean surfaces, the satellite takes one daytime and one night-time measurement of the surface temperature.

The time series of 120 monthly *Chl-a* and SST composites were assembled from the http://gdata2.sci.gsfc.nasa.gov/daac-bin/G3/gui.cgi?instance_id=ocean_month on November 2012. The tool for the *Chl-a* and SST data extraction was the Interactive Online Visualization and Analysis Infrastructure (GIOVANNI), a web-based application developed by the Goddard Earth Sciences Data and Information Services Center (GES DISC). Giovanni was used to assemble the time series (ASCII format and satellite imagery) at the Ocean Colour Radiometry Instance. A detailed description of the procedures for data extraction using GIOVANNI is provided by Berrick et al. (2004). The time series were used for the

calculation of the statistical characteristics (mean and standard deviation) and anomalies aiming at the interpretation of the seasonal cycle and interannual variability. Wavelet analysis was performed in the time series with the aim of extracting the main periodicities in the variability of the weekly and monthly *Chl-a* and monthly SST.

3.3.2. Sea surface wind and data processing

Sea surface wind (SSW) plays a key role in regulating the earth's water and energy cycles and redistribution of chemical and other properties (e.g. CO_2) between the atmosphere and the ocean (Zang et al., 2006). The SSW has a large application e.g. to compute air-sea fluxes, biophysical interactions and climate studies. Traditionally the winds are measured using anemometers, ships, weather buoys and scatterometers on-board satellites. On-board the satellites winds are measured using a microwave radar scatterometer where a radar signal is transmitted to the surface of the ocean and then it is backscattered to the sensor. The roughness of the sea surface influences the strength of the signal and is used to determine the relative direction and speed of wind acting on the surface of the ocean. Winds are measured with a microwave radar scatterometer where a radar signal is transmitted to the surface of the ocean and then is backscattered to the sensor (Zang et al., 2006).

Blended winds from different instruments provide better resolution data by filling the temporal and spatial gaps in data from the individual instrument observations. Blended wind data sets from continuous observations of multiple satellite sensors, such as the Advanced Microwave Scanning Radiometer–Earth Observation System (AMSR-E), Spatial Sensor Microwave Image (SSMI)-F13, SSMI-F14, SSMI-F15, Quick Scatterometer (QuikSCAT) and Tropical Microwave Image (TMI) are available from the NOAA/NCDC (http://www.ncdc.noaa.gov/oa/rsad/air-sea/seawinds.htm/).

In this study we use daily and monthly blended sea surface wind speed ($m.s^{-1}$) and wind velocity vector components (*u* and *v*) at a reference height of 10 m, with spatial resolution of 0.25^{o} (720 bytes latitude x 1440 bytes longitude). The level 3 wind data was downloaded from NOAA/NCDC on the 05 April 2013 as network Common Data Form (NetCDF) files from http://www.ncdc.noaa.gov/oa/rsad/air-sea/seawinds.htm. These wind data were used to assess the prevailing SSW and its relationship with the *Chl-a* during 2003-2012.

The daily wind data extracted from the NetCDF files was averaged into weekly and monthly time series. Then the time series were used for the calculation of the statistical characteristics (mean, standard deviation) and anomalies aiming at the interpretation of the seasonal cycle and interannual variability. Wavelet analysis was performed in the daily, weekly and monthly time series of the wind speed.

3.3.3. Satellite altimetry and data processing

Altimetry is a technique used in remote sensing for measuring the ocean surface height using the electromagnetic radiation in the microwave bands. The time a radar pulse takes to travel from a satellite antenna to a surface and get back to the satellite receiver is the basis for satellite altimetry measurement (http://www.aviso.oceanobs.com). The data, which has to be carefully corrected for a variety of geophysical processes, is then fundamental in helping to determine sea surface heights from which sea surface height anomaly (SLA) can be derived, e.g. http://www.aviso.oceanobs.com/en/data/index.html. Satellite altimetry data is important for the characterization of mesoscale eddies (Chelton et al., 2007). For the southern hemisphere negative SLA represents cyclonic (clockwise rotation) eddies whereas positive SLA represents anti-cyclonic (anti-clockwise rotation) eddies (Halo et al., 2014).

The merged altimetry data product improves the estimation of mesoscale signals. The satellite altimetry data used in this study is available from SSALTO/Duacs and is distributed by AVISO with support from Centre National d'Etudes Spatiales (CNES) (http://www.aviso.oceanobs.com). The data which have a spatial resolution of 0.33^{o} is a product merged from multi-satellite altimeter missions which comprise TOPEX/Poseidon, ENVISAT, GFO, Jason-1, ERS-1 and ERS-2 and it is provided on a Mercator projection. We use gridded weekly maps of sea level anomalies (SLA) from 2003 to 2012 to assess the mesoscale eddies variability in Delagoa Bight.

Contrary to the *Chl*-a, SST and SSW data, the presentation of the SLA data consisted of the use of weekly maps to illustrate selected events during the study period. This choice was based on the fact that the SLA time series for the Delagoa Bight averaged area presented very low values. These values were further reduced on averaging to monthly means in

order to be comparable to the *Chl-a*, SST and SSW. The values being small we decided that the weekly maps could illustrate better the SLA. According to Halo et al. (2014) the Delagoa Bight is an area of high mesoscale cyclonic and anticyclonic eddies variability. For illustrative purposes we used daily and weekly composite plots from Level 3 *Chl-a* concentration and SST data available at Colorado Center Astrodynamics Research (CCAR), (http://eddy.colorado.edu/ccar/data_viewer/index).

Time series statistical and wavelet analysis

The data processing and plotting of the time series of *Chl-a* concentration, water temperature and SSW were performed using the programming language Matlab R2012a (http://www.mathworks.com/products/matlab/) and the Microsoft Excel 2010 (https://products.office.com/en-us/excel). For the interpretation of the seasonal and interannual variability, the seasons for the southern hemisphere were defined as summer (January, February and March- JFM), autumn (April, May and June- AMJ), winter (July, August and September- JAS) and spring (October, November and December- OND). Anomalies were calculated for each variable by subtracting the extracted value from the mean (of the same month for all years) for each month to investigate the seasonal variations.

The statistical analysis (mean, standard deviation (STD), Skewness, Kurtosis and the correlations) were calculated according the equations 3.1-3.6, where *X* and *Y* are the variables, *n* is the total number of data records and *i* is the data index (Thomson and Emery, 2014).

$$Mean = \frac{\sum X}{n} \qquad \text{(eq.3.1)}$$

$$Variance(X) = \frac{\sum X^2 - \frac{\left(\sum X\right)^2}{n}}{n} \qquad \text{(eq. 3.2)}$$

$$STD(X) = \sqrt{Variance\ (X)} \qquad \text{(eq. 3.3)}$$

$$Skewness = \frac{\sum_{i=1}^{n}(\boldsymbol{Y_i}-\bar{\boldsymbol{Y}})^3}{(n-1)s^3} \qquad \text{(eq 3.4)}$$

$$Kurtosis = \frac{\sum_{i=1}^{n}(Y_i-\bar{Y})^4}{(n-1)s^4} \qquad \text{(eq 3.5)}$$

The Skewness is a measure of how symmetrical the data set is distributed. A symmetrically distributed data set has a Skewness of zero. The Kurtosis determines if a data set has a peak or is flat relative to the normal distribution (http://www.itl.nist.gov/div898/handbook/eda/section3/eda35b.htm).

The linear relationship, expressed by the correlation coefficients between the time series, was calculated using the *Pearson product moment correlation coefficient* (eq 3.6) which gives the strength and direction of the relationship between two continuous dependent (X) and independent (Y) variables.

$$r = \frac{n\sum XY-(\sum X)(\sum Y)}{\sqrt{[n\sum X^2-(\sum X)^2][n\sum Y^2-(\sum Y)^2]}} \qquad \text{(eq 3.6)}$$

r is a dimensionless quantity varying from -1 $\leq r \leq$ +1. A correlation greater than 0.8 between *X* and *Y* is generally described as strong and a correlation less than 0.5 is weak (Thomson and Emery, 2014). A correlation is statistically significant when the p-value is in the range 0.01 or 0.05, which gives the evidence that the null hypothesis can be rejected and thus it can be concluded that there is a relationship between the variables X and Y. The *r-squared* value represents the proportion of variance in the dependent variable that is explained by the independent variable.

Wavelet analysis

Wavelet analysis is a signal processing technique that addresses the constraints presented by the Fourier transform in the processing of non-stationary signals (Torrence and Compo, 1998). Fourier analysis is a mathematical technique for transforming a signal from a time-based to a frequency-based domain which makes it more suitable for characterizing stationary processes (Lau and Weng, 1995; Torrence and Compo, 1998). The Fourier analysis inability to detect the non-stationary or transitory characteristics of a signal (e.g.

drift, trends and abrupt changes) is a drawback addressed by the wavelet analysis, which decomposes a signal into time-frequency domain (Torrence and Compo, 1998).

A detailed description of wavelet analysis including illustrative examples is provided by Torrence and Compo (1998). Wavelet analysis have been used in the Ecology and Oceanography for the investigation of the main periodicities in time series (Winder and Cloern, 2010; Malauene et al., 2014). In this research we use the Morlet wavelet which provides a good balance between time and frequency localization. The Morlet function is essentially a damped complex exponential, which can capture local (in time) cyclical fluctuations in the time series (Torrence and Compo, 1998). Further aspects of the wavelet analysis using the Morlet method are described in detail by Torrence and Compo (1998) (http://paos.colorado.edu/research/wavelets/).

The wavelet analysis was performed into the time series of *Chl-a*, SST, wind speeds and UTR data. Prior to performing the wavelet analysis the seasonal cycles has to be removed from each time series through the normalization by subtraction of the mean and division by the standard deviation, making the mean zero. Therefore the wavelet analysis was not performed for the zonal and meridional wind components and to the sea level anomalies to avoid the misinterpretation of the results.

The Equation 3.1 was used to average the data into daily, weekly and seasonal means. According to the case the seasonal cycle in the time series was removed by subtracting each monthly (and seasonal) value from its respective monthly (and seasonal) average calculated for the data range period. The same procedure was used to calculate the seasonal means from the monthly *Chl-a*, SST and SSW.

CHAPTER FOUR - RESULTS

In this chapter we present the results which are structured in three main sections: Section 4.1- Seasonal variability of *Chl-a* concentration, SST and SSW; Section 4.2- Interannual variability of *Chl-a* concentration, SST, SSW and SLA and; Section 4.3- *In situ* water temperature and cool coastal water events at Ponta Zavora. The *Chl-a*, SST and SSW results presented here are based, mainly, in the analysis of time series. A different approach was chosen for the SLA. Due to the very low values observed in the SLA time series for the Delagoa Bight averaged area, we made a choice to use weekly maps to illustrate selected events depicted from the other variables.

4.1. Seasonal variability of *Chl-a,* SST and SSW

The seasonal pattern of *Chl-a* concentration, SST and SSW represented by the 10-year (2003-2012) climatological monthly composites for the Delagoa Bight (24-28^{o}S, 32-36^{o}E) averaged area are presented in Figure 4.1. The surface *Chl-a* is the primary variable for this study. Figure 4.1 and Figure 4.2a show the *Chl-a* concentration (imagery and time series) measured in mg.m^{-3} and presented in the log scale.

The seasonal *Chl-a* variability (Figure 4.1) exhibited a spatial pattern of inshore-offshore gradient with elevated *Chl-a* concentration (>0.5 mg.m^{-3}) distributed along the coastal waters (shallower depths), whereas the majority of the bight exhibited *Chl-a* concentration of ~0.5 mg.m^{-3}. Oligotrophic conditions (*Chl-a* ~0.1 mg.m^{-3}) were noticeable off the shelf (deep waters), except during July-August, when the inshore-offshore *Chl-a* gradient weakened due to the increase in the offshore *Chl-a* concentration to ~0.22 mg.m^{-3}. The seasonal cycle, with an amplitude of ~0.25 mg.m^{-3}, exhibited a temporal pattern of increasing *Chl-a* concentration from June through September (late autumn - late winter) and a decreasing pattern from December to May (late spring - mid autumn). The timing of the seasonal minimum (0.14 mg.m^{-3}) and seasonal maximum (0.39 mg.m^{-3}) were December and August, respectively, as seen in Figure 4.2a.

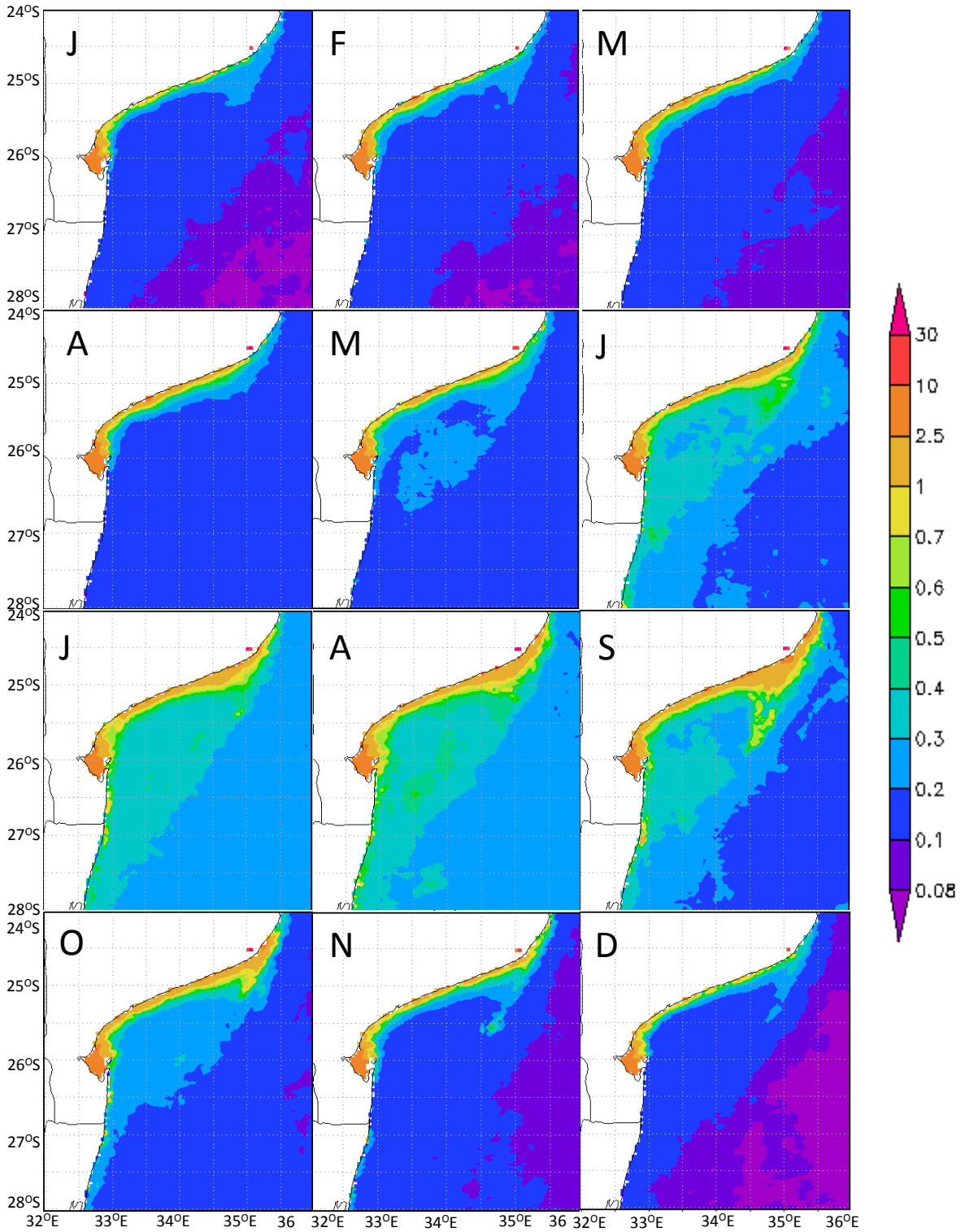

Figure 4.1:Monthly climatological maps (2003-2012) of MODIS Aqua *Chl-a* concentration for the Delagoa Bight (24-28°S, 32-36°E). Elevated Chl-a concentration occurred from June through October with the maximum in August. The purple and red colours in the colour bar represent low and high *Chl-a* values, respectively.

Extending the analysis to the monthly climatology of the SST and SSW, Figure 4.2 shows distinct patterns of variability. The SST monthly climatology, Figure 4.2(b), exhibits a strong SST seasonal cycle with amplitude of ~5^{o}C. The SST seasonal minimum was 22.4^{o}C whereas the SST seasonal maximum was 27.4^{o}C. The surface water temperatures, shown in Figure 4.2b, decreased from April to September (mid autumn - late winter) and increased from October to May (early spring - early autumn). The SST monthly climatological maps (not shown) exhibited a quasi-uniform gradient between the inshore and offshore waters.

Surface forcing variability indicated by the wind vectors (zonal and meridional components) (Figure 4.2c and Figure 4.2d respectively) suggested the predominance of the onshore seasonal winds throughout the year. The zonal wind component magnitude was at its maximum in July (~3.2 m.s^{-1}) and its minimum in November (~2.5 m.s^{-1}) with relatively low amplitude of ~0.7 m.s^{-1}. The magnitude of the climatological meridional wind component reached a maximum (~2.6 m.s^{-1}) in July and a minimum (~1.4 m.s^{-1}) in January. It is worth noting the absence of the alongshore NE (north-east) winds which are the upwelling favourable winds for Delagoa Bight.

The analysis of the overall climatological fields (Figure 4.2) shows that the concurrent conditions that triggered the timing of the seasonal maximum *Chl-a* concentration in mid winter (August) were the drop in surface water temperatures to a minimum of ~22.4^{o}C, and the prevalence of onshore winds. The zonal and meridional wind components (Figure 4.2 a, c and d) reached their maximum magnitudes in July, one month earlier than the seasonal maximum *Chl-a* concentration, suggesting a time lag of one month with the wind preceding the *Chl-a* concentration.

The comparison between the seasonal field patterns shows that the *Chl-a* concentration and SST climatological fields (Figure 4.2a and Figure 4.2b) exhibited a clear seasonal cycle contrasting with the fields of the wind vectors (Figure 4.2c) and the wind speed (not shown) which did not exhibit a clear seasonal cycle during 2003-2012. The quarterly seasonal cycles (averages for JFM, AMJ, JAS and OND) for the *Chl-a* concentration, SST and SSW fields for 2003-2012 (not shown) exhibited slightly similar patterns depicted in the monthly seasonal cycles.

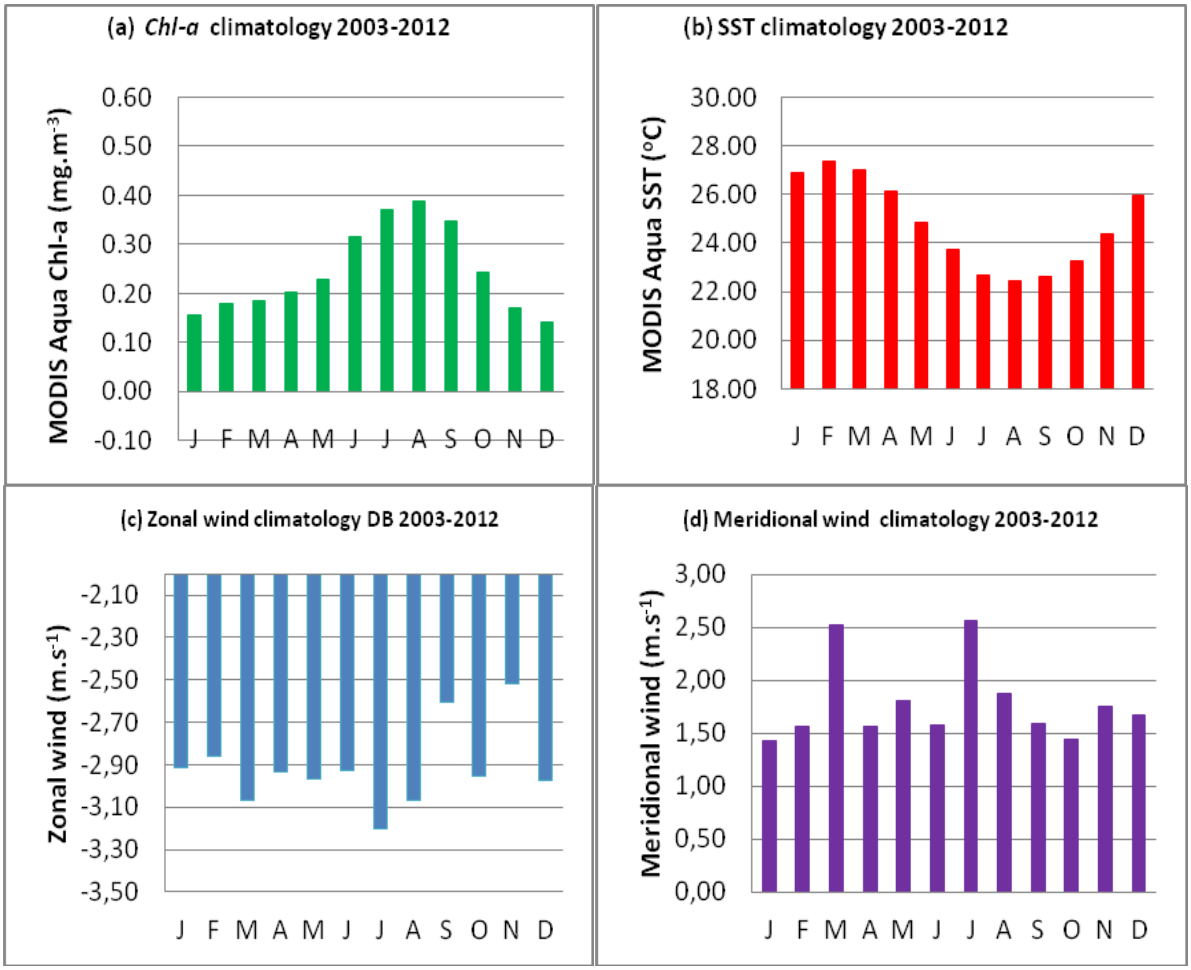

Figure 4.2: Ten years of climatological mean fields of (a) 4 km resolution MODIS Aqua Chl-a, (b) MODIS Aqua SST, multi-satellite winds (0.25o resolution) for (c) zonal and (d) meridional wind components during 2003-2012 in the Delagoa Bight (24-28°S, 32-36 ° E).

4. 2. Interannual variability of *Chl-a*, SST and SSW

4. 2.1. Frequency distribution of *Chl-a*, SST and SSW

The histograms of the monthly time series of *Chl-a*, SST and SSW (zonal and meridional wind components) are presented in Figure 4.3. The *Chl-a* concentration and the zonal wind component histograms (Figure 4.3a, Figure 4.3c and Figure 4.3d) are relatively skewed towards the positive values (right skewed) suggesting the existence of numerous events with higher values than the mean for each time series.

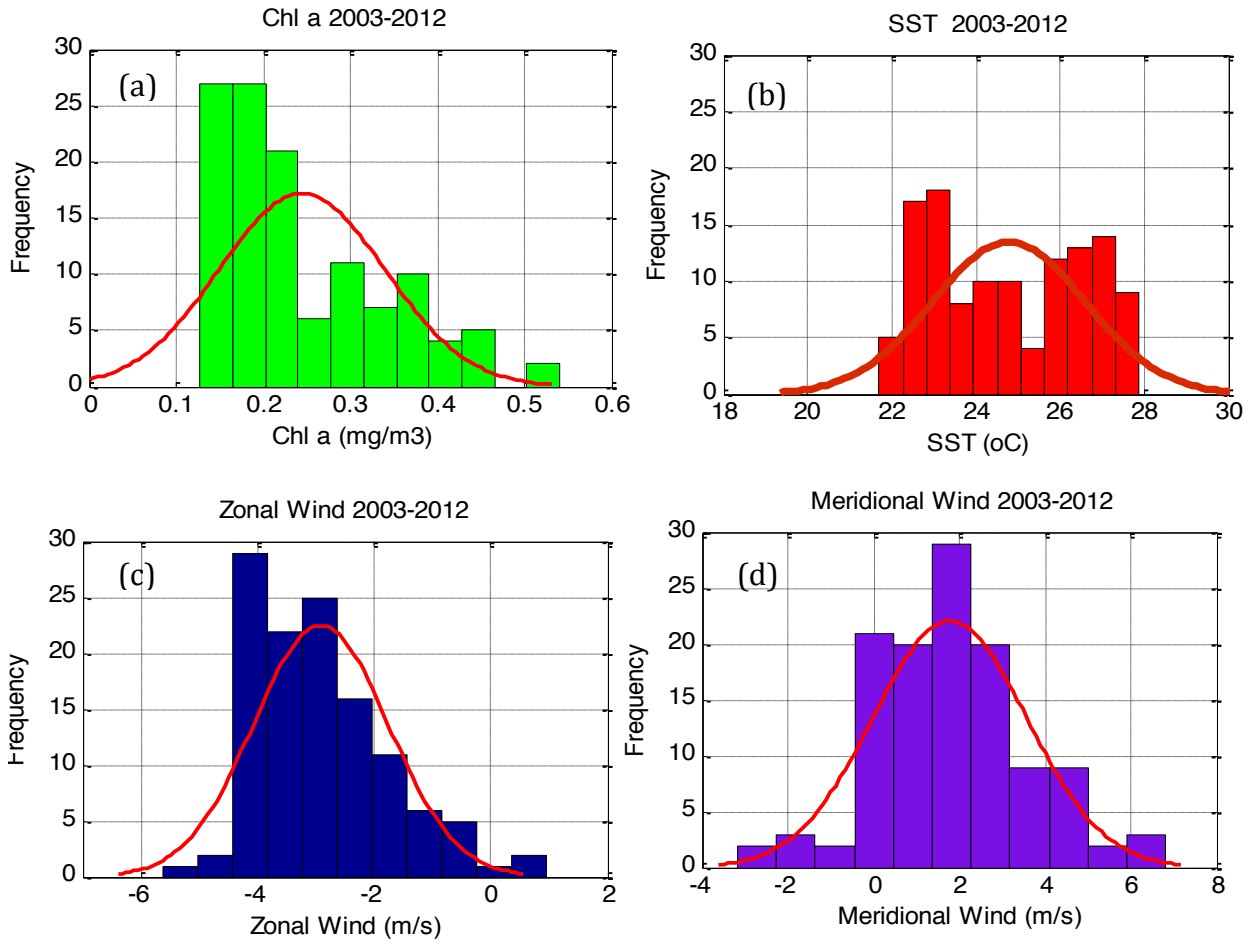

Figure 4.3: Frequency histograms with the normal fit (red line) of (a) Chl-a, (b) SST, (c) Zonal wind and (d) meridional for the Delagoa Bight during 2003-2012.

4.2.2. Monthly time series of *Chl-a*, SST and SSW

The temporal evolution of the *Chl-a*, SST and SSW fields from the monthly time series for the Delagoa Bight averaged area during 2003-2012 are presented in Figure 4.4. The surface *Chl-a* monthly mean (Figure 4.4 a) ranged from 0.13 $mg.m^{-3}$, in 2009 (December), to 0.54 $mg.m^{-3}$, in 2003 (August), with an amplitude of ~0.41 $mg.m^{-3}$. The *Chl-a* long term (2003-2012) mean was ~0.24 ± 0.10 $mg.m^{-3}$. There was a general pattern of *Chl-a* peaks in winter and troughs in summer. The interannual variability showed that the timing of the most prominent *Chl-a* peaks (Figure 4.4a) shifted from June, July, August to September whereas the interannual minimum was more stable and shifted from December to January. The

comparison among the 10-year variability values showed 2004, 2008, 2009 and 2010 as the years with lower *Chl-a* than those of 2003, 2005, 2006, 2007, 2010, 2011 and 2012.

The monthly SST (Figure 4.4b) exhibited a strong seasonal cycle of cooling from April to September and warming from October to March. The monthly mean SST (Figure 4.4b) ranged from 21.7^{o}C, in 2011 (July), to 27.9^{o} C, in 2006 (February) with an amplitude of ~6.2^{o}. The SST long term (2003-2012) mean was ~24.8±1.92^{o}C. The timing of the SST minimum shifted from July, August to September whereas the timing of the maximum shifted from January, February to March. The years 2004, 2008 and 2012 were cooler than 2003, 2005, 2006, 2007, 2009, 2010 and 2011. The SST interannual variability, taken from the horizontal maps (not shown), exhibited a slightly uniform inshore-offshore gradient compared to the latitudinal gradient of ~3^{o}C, with the northern Delagoa Bight warmer that the southern region.

The monthly wind vectors are illustrated in Figure 4.4c and the wind speed in Figure 4.4 (d). The wind vectors (Figure 4.4c) indicate the onshore direction prevailing over the 10–years period. The wind vectors were relatively stronger (~3.5 m.s^{-1}) during 2003-2006 than in the other years. Sporadic NE winds (upwelling favorable winds for Delagoa Bight region) were observed, for example from late 2008 to mid 2011 as depicted in Figure 4.4c. The monthly mean wind speeds (Figure 4.4d) ranged from ~1.0 m.s^{-1}, in 2007 (January), to ~ 8.0 m.s^{-1} in 2004 (July) with the (2003-2012) long term mean speed of ~4.0 ±1.35 m.s^{-1}. Figure 4.2a and Figure 4.2b display a strong seasonal cycle in the *Chl-a* and SST time series, while the wind vectors (Figure 4.4c) and wind speed (Figure 4.4d) lack a clear seasonal cycle.

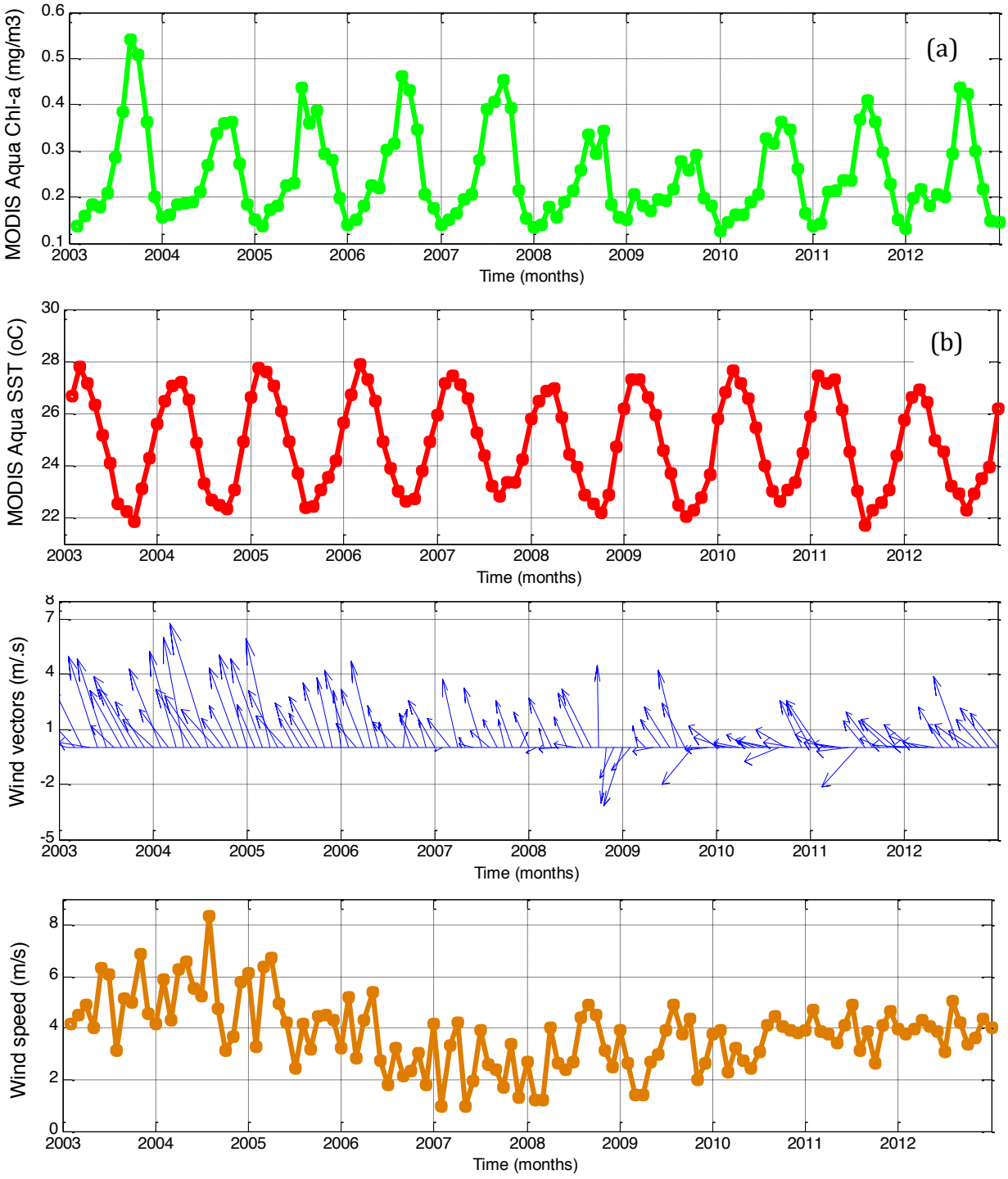

Figure 4.4: Time series of monthly composites of (a) Chl-a concentration, (b) SST, (c) wind vectors and (d) wind speed for the Delagoa Bight during 2003-2012.

To summarise the significant time scales of variability in the time series of *Chl-a*, SST and wind speed a wavelet analysis was applied to the time series of 120 monthly data with the

mean not removed (Figure 4.5, Figure 4.6, Figure 4.7). The wavelet power spectrum, denoted *b* in Figure 4.5 Figure 4.6 and Figure 4.7, shows the decomposition of the series in time (along the *x*-axis) and period (along the *y*-axis). The dashed white line in these figures is the cone of influence (COI) which represents the region of edge effects resulting from the loss in statistical power near the start and the end of the time series. The global wavelet spectrum shows the thick contours enclosing the area of greater than 95% for a red-noise process with a lag-1 coefficient of 0.72 (Torrence and Compo, 1998). The colour bar shows high intensity variance (dark red) and low intensity (dark pink). Y-axis is the period (days) and x-axis is the time (days) of recurrent strength of the periods.

The strong *Chl-a* and SST seasonal signals apparent from the Figure 4.4a and Figure 4.4b are further confirmed by the wavelet analysis which display a recurrent annual cycle (shown in red). The ~12-month time-averaged spectrum, (Figure 4.5, Figure 4.6, Figure 4.7) showed that this periodicity was highly significant and explained the largest proportion of the variance in both *Chl-a* and SST time series. While for the SST time series the signal is present throughout the 10 years, for the *Chl-a* it was absent during 2009.

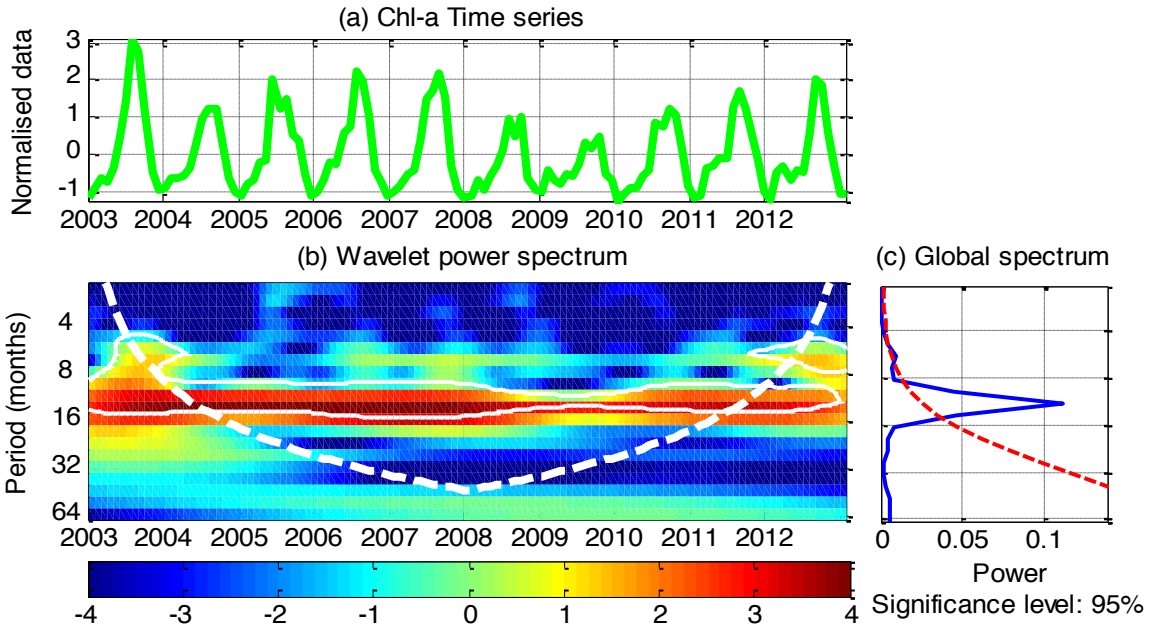

Figure 4.5: a) *Chl-a* concentration time series, (b) wavelet power spectrum, (c) global wavelet spectrum with thick contours enclosing area of greater than 95% for a red-noise process. (Torrence and Compo, 1998). The cone of influence (dashed white line in b) is the region of edge effects resulting from the loss in statistical power near the start and the end of the time series.

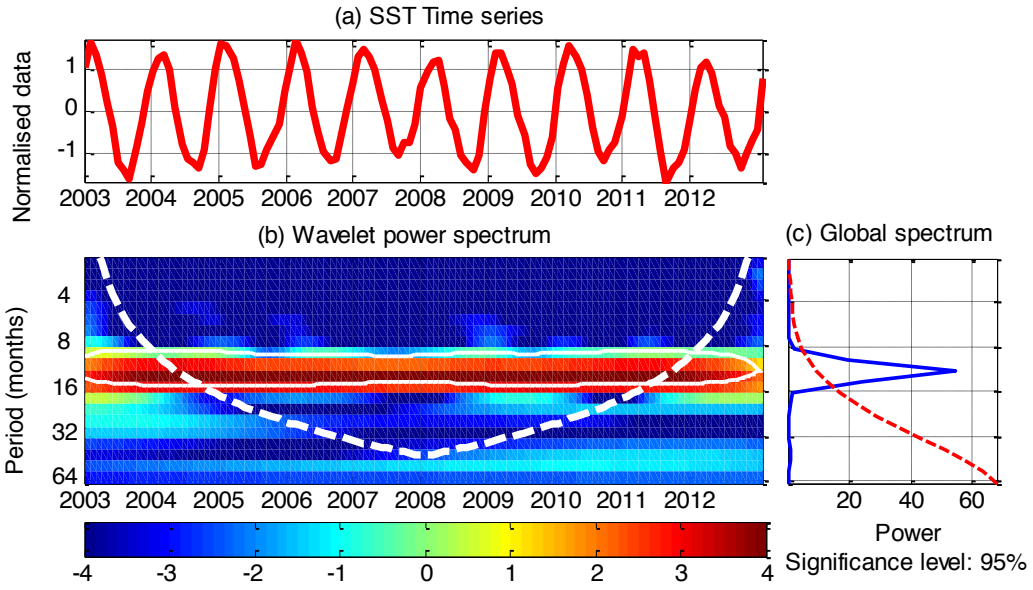

Figure 4.6: (a) SST time series, (b) wavelet power spectrum, (c) global spectrum with thick contours enclosing area of greater than 95% for a red-noise process (Torrence and Compo, 1998). The cone of influence (dashed white line in *b*) is the region of edge effects resulting from the loss in statistical power near the start and the end of the time series.

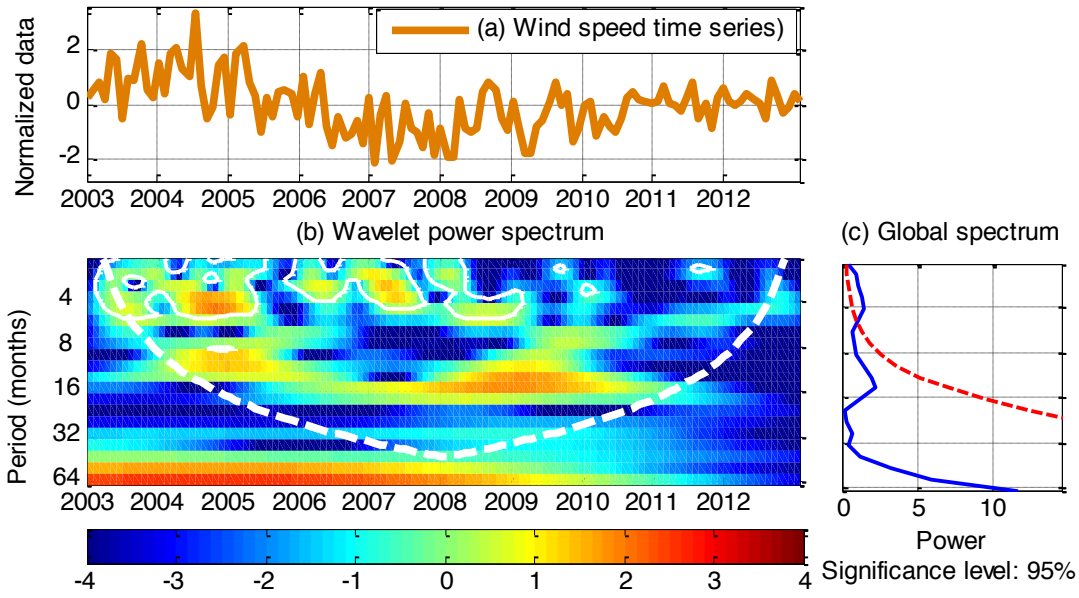

Figure 4.7: (a) Wind speed time series, (b) wavelet power spectrum, (c) global wavelet spectrum with thick contours enclosing area of greater than 95% for a red-noise process (Torrence and Compo, 1998). The cone of influence (dashed white line in *b*) is the region of edge effects resulting from the loss in statistical power near the start and the end of the time series.

4.2.3. Monthly anomalies time series of Chl-a SST and SSW

The non-seasonal variations (anomalies) obtained by subtracting the mean seasonal cycles from the monthly time series of *Chl-a*, SST and SSW are shown in Figure 4.8. The magnitude of the *Chl-a* concentration anomalies (Figure 4.8a) ranged from -0.13 $mg.m^{-3}$, in 2009 (August) to 0.16 $mg.m^{-3}$, in 2003 (September). Events of persistent *Chl-a* positive anomalies were observed, e.g. in July 2003- February 2004 and March-August 2006, April-September 2007 and February- July 2011(Figure 4.8a), whereas persistent negative events were observed e.g. during October 2007- November 2008 and March 2009- January 2011. A consistent pattern of *Chl-a* anomalies was observed during 2011, with negative anomalies occurring during summer-autumn whereas positive anomalies occurred during winter-spring. Synchronized positive *Chl-a* and negative SST anomalies (indication of upwelling) occurred with irregular timing and magnitude during 2003-2012 (Figure 4.8a and Figure 4.8b).

The SST monthly anomalies (Figure 4.8b) ranged from -1.19 ^{o}C in 2012 (April) to 0.78 ^{o}C in 2005 (January). Figure 4.8b shows periods of persistent positive SST anomalies with an average warming of ~0.2 - 0.4^{o}C above the long term SST mean, e.g. during February 2006 - October 2008, February- November 2010. Conversely, there were intermittent SST negative anomalies (indication of upwelling) representing an average cooling of ~0.5-1.0 ^{o}C below the long term SST mean, e.g. during July 2003 - February 2004, February 2009 - January 2010 and April 2011- June 2012 (Figure 4.8b). The monthly anomalies (Figure 4.8a and Figure 4.8b) suggest episodic periods of synchronized events of positive *Chl-a* and negative anomalies, e.g. during July 2003 - March 2004.

The wind vectors anomalies during 2003-2012 exhibited two main modes of variability. From January 2003- June 2009 the prevailing winds were blowing towards the shore while during July 2009- May 2012 they were predominantely blowing from NE towards SW (Figure 4.8c). The maximum wind magnitude (~5.0 m.s^{-1}) was registered in 2004, for the winds blowing towards the shore and in 2008, for the winds blowing from NE towards the SW.

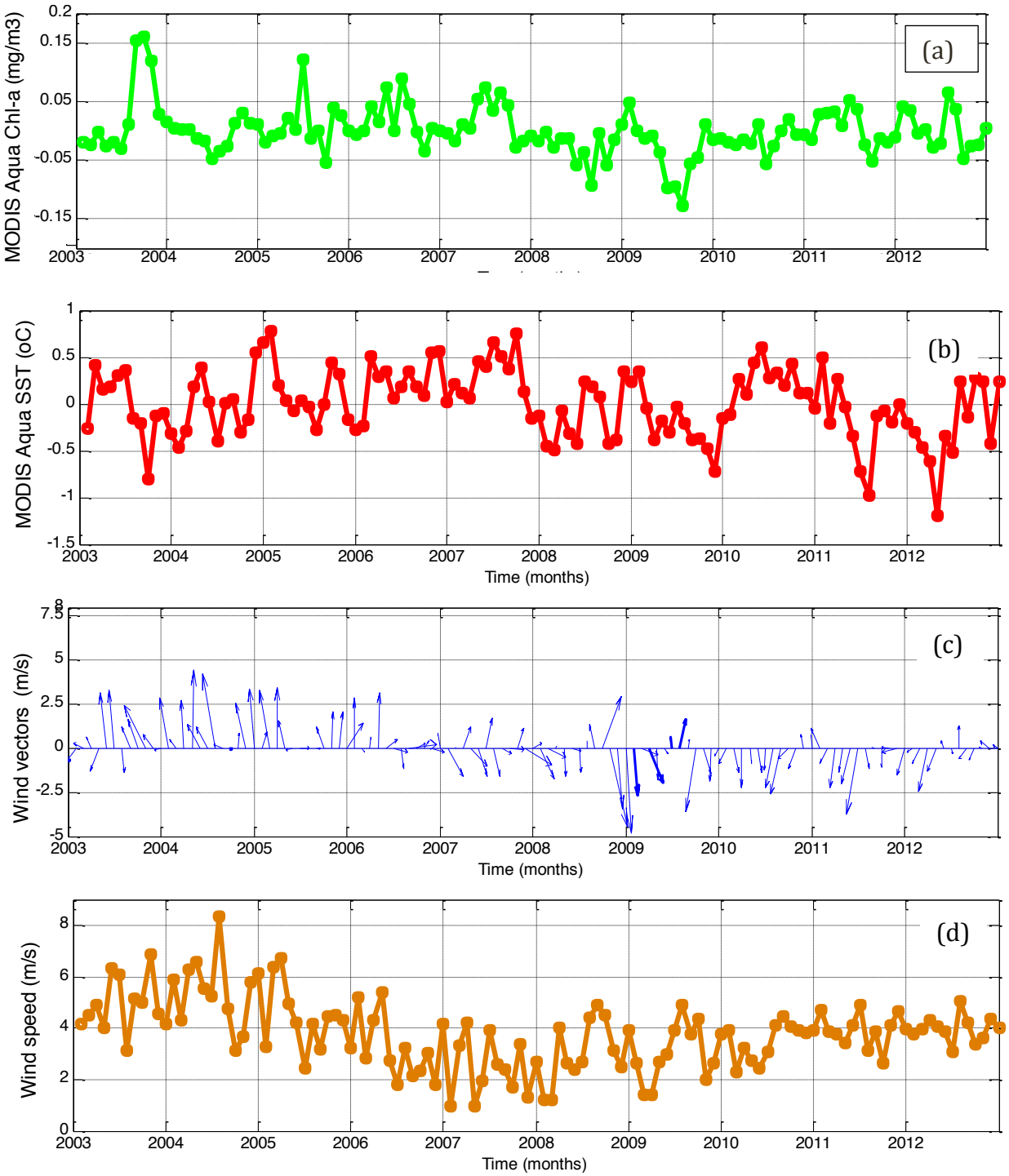

Figure 4.5: Time series of monthly anomalies of (a) Chl-a concentration, (b) SST, (c) wind vectors and (d) wind speed for the Delagoa Bight from January 2003 to December 2012.

In the next section we further examine the variability of *Chl-a*, SST and SSW (wind vectors and speed) anomalies by selecting two periods from Figure 4.8: July 2003 to March 2004,

the period of the relatively higher *Chl-a*, and (ii) August 2009- April 2012, the period of the persistent coastal upwelling favourable winds (NE). The reasoning for choosing July 2003 - Mar 2004 was to examine whether there was a coherence between the *Chl-a,* SST, SSW during the anomalous *Chl-a* event while for the period August 2009- April 2012 the aim was to examine the biological response and the SST variability during the persistent NE winds.

4.2.3.1. Anomalous event of high *Chl-a*

Figure 4.9 illustrates the variability of the *Chl-a*, SST and SSW during July 2003-March 2004. The *Chl-a* concentration anomaly registered a modest increase from July to October 2003 followed by a decrease throughout March 2004. The Maximum *Chl-a* anomaly (0.16 $mg.m^{-3}$) registered in September was concurrent with SST anomaly of ~0.8 ^{o}C. From January to October 2004 the SST and the *Chl-a* anomalies were varying in opposite while the the winds were blowing towards the shore with relatively low speeds of ~2.5 $m.s^{-1}$ Figure 4.9).

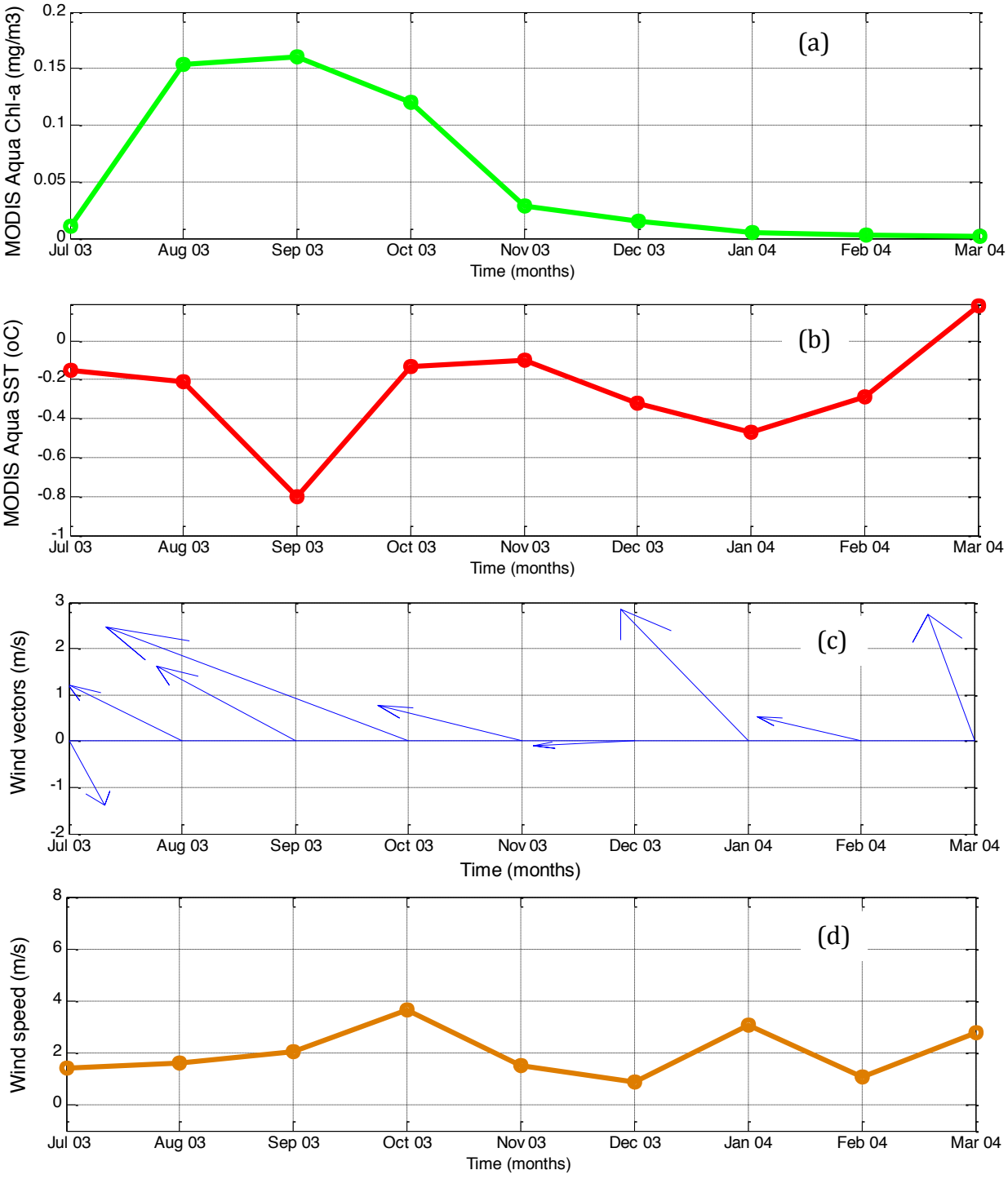

Figure 4.6: Monthly anomalies of (a) Chl-a concentration, (b) SST, (c) wind vectors and (d) wind speed during July 2003 - March 2004 in the Delagoa Bight (24-28°S, 32-36°E).

A mosaic of six weekly maps from AVISO illustrates the variability of the sea level anomalies (SLA) in the Delagoa Bight region during July 2003- March 2004 (Figure 4.10). the SLAs variation was low and ranged from -0.5 to 0.5 cm. Within the study domain (24-28^{o}S, 32-36^{o}E), the SLAs in the western region (near the land) were comparatively higher than those on the eastern side (seawards). A cyclonic-like structure (negative SLA for the southern hemisphere) was apparent from the south-east region od Delagoa Bight and seemed to be evolving from the south-east domain towards the west (land side) (Figure 4.10a). From the 30 July 2003 the the horizontal displacement of the structure within the study domain was ~100 km (~35- 36^{o}E) while in the week of 29 October 2003 (Figure 4.10b), it was found at ~34.3-36^{o}E, representing a horizontal displacement of ~150 km.

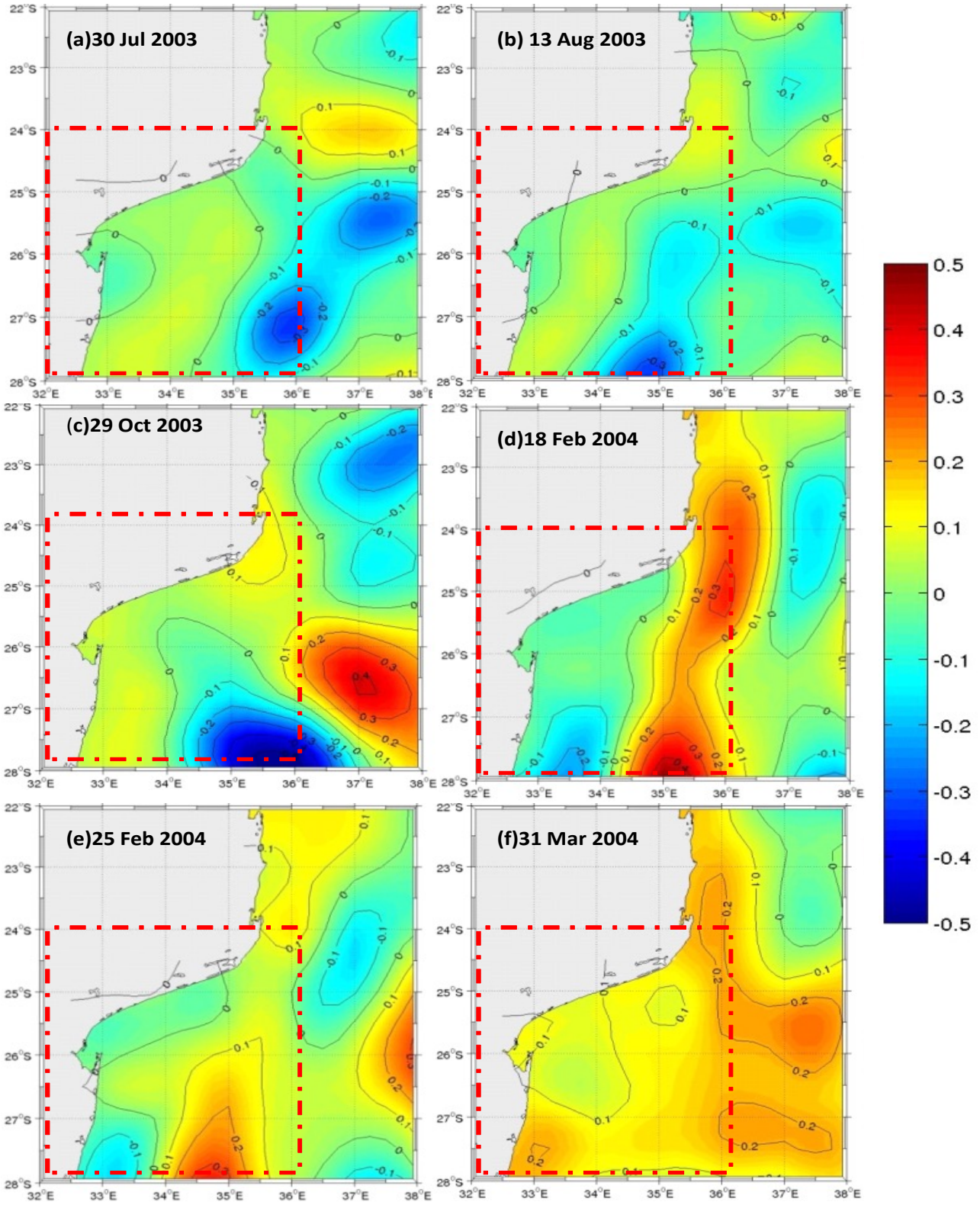

Figure 4.7: Selected weekly maps of SLA from AVISO during the longest event of synchronized anomalies of positive Chl-a and negative SST (July 2003-March 2004), in the Delagoa Bight. Note the prevalence of relatively low (-0.5 to 0.5 cm) SLA in the study domain (22-28°S, 32-38°E, dashed red rectangle).

4.2.3.2. Persistent NE winds during August 2009- April 2012

The *Chl-a*, SST and SSW (wind vectors and speed) observed during August 2009- April 2012 in the Delagoa Bight are illustrated in Figure 4.11. The prevailing winds were blowing from NE (noth-east) towards the SW (south-west) (Figure 4.11c). Due to the orientation of the Delagoa Bight coast and according to the Ekman transport theory the NE winds are the coastal upwelling favourable winds. Generally, the occurrence of these NE winds did not induce a significant increase of *Chl-a* concentration (Figure 4.11a and Figure 4.11c). Contrary to the *Chl-a c*oncentration, the SST anomalies semmed sligthly coherent with the NE winds indicated by the bold arrows in Figure 4.11c. Generally, the NE wind anomalies were associated to relatively high wind speeds anomalies.

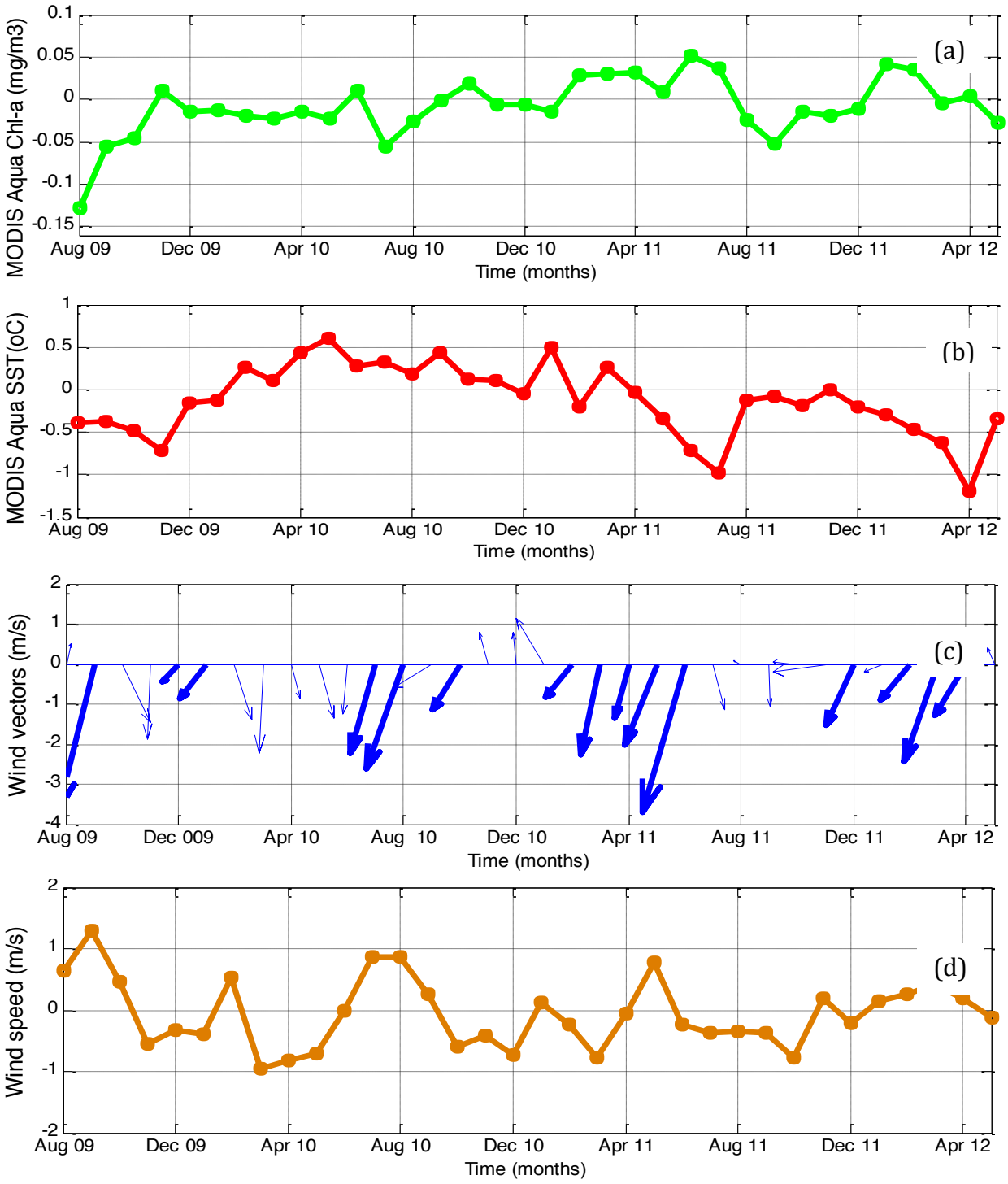

Figure 4.8: Monthly anomalies of (a) Chl-a concentration, (b) SST, (c) wind vectors and (d) wind speed during August 2009 - May 2012. The upwelling favourable winds for Delagoa Bight region is from NE (north-east) towards SW (south-west) as indicated by the bold arrows in 4.11c.

4.2.3.3. Correlations between Chl-a, SST and SSW in the Delagoa Bight

An attempt to assess the linkages between the *Chl-a* and the *SST,* SSW and SLA during the study period was made by calculating the correlation coefficients between the *Chl-a* and the SST, SSW (zonal and meridional component and wind speed) and the SLA, using monthly and monthly anomalies time series. Due to a mismatch in the length of the time series (the SLA data is up to August 2012) the correlations were calculated for the period January 2003 - December 2011.

The time series were normalized prior to the correlations calculations. The statistically significant correlation was indicated by $p<0.05$. According to the results (not shown) there was a general lack of significant correlations between the *Chl-a* and the physical variables when the correlations were calculated using the long term (2003-2011) time series of monthly anomalies. An attempt to calculate the correlations at the year-to year basis showed weak but significant correlations (not shown). Exceptionally, during 2009, there were moderate and statistically significant correlations between the anomalies of *Chl-a* and the zonal wind component (-0.63, p-value 0.029) and between the *Chl-a* and the wind speed (0.63, p-value 0.026). Furthermore, the 2009 monthly time series showed the only statistically significant positive correlation (0.59, p-value 0.043) between the *Chl-a* and the wind speed in the 10-years time series.

The monthly means fields of the *Chl-a*, SST, SSW (Figure 4.4) and maps of weekly SLA (Figure 4.10) depict distinct patterns of variability with synchronized events of negative anomalies of SST and positive anomalies of *Chl-a* (an indication of upwelling events) being observed during 2003-2012. In the next section, we investigate the occurrence of cool water events in the northern Delagoa Bight using Ponta Zavora (24.48° S, 35.24° E) as a case study.

4.3. *In situ* water temperature and cool water events at Ponta Zavora

4.3.1. Water temperature variability at Ponta Zavora

A ~5-year time series of *in situ* water temperatures recorded at 17 m depth at Ponta Zavora is used to investigate the water temperature variability and the cool water events in the northern Delagoa Bight. Cool water events are defined as a decrease of ~2°C in the water temperature. Figure 4.12 shows the histogram of the 5-year period time series of daily temperatures re-sampled by averaging from 24 hourly records.

The time series of 1856 samples registered a daily mean temperature of 23.98 ±1.99 °C. The water temperature dataset is non- symmetrically distributed, Skewness ~0.14, and has a Kurtosis of ~2.26, the latter indicating the position of the peak relative to the normal distribution (red line).

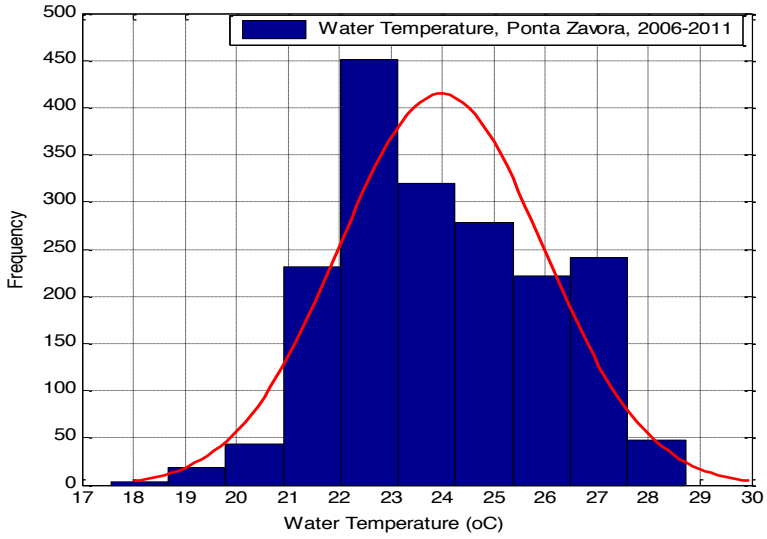

Figure 4.9: Time series histogram with the normal fit (red line) of the water temperature data set recorded at 17m depth in the northern shore of Delagoa Bight at Ponta Zavora from April 2006 to May 2011.

Figure 4.13 depicts a dominant seasonal cycle with cool water temperatures occurring from May to September, whereas warm water temperatures occurred from October to March. Note that the UTR was deployed from 23 April 2006 to 22 May 2011 therefore 2006 and 2011 have data records for 253 and 142 days respectively.

The water temperature amplitude over 5-years was ~11.14°C, with the minimum (~17.56°C) recorded on 09 October 2009 and the maximum (~28.70°C) on 25 January 2011. A year to year variability (Figure 4.13) showed 2009 as the year of the highest amplitude (~10.2°C), whereas 2007 registered the lowest amplitude (~7.2°C). The blue dashed rectangles in Figure 4.13 highlight some of the cool water events (~2°C decrease) observed in the northern Delagoa Bight during 2006- 2011.

The maximum and minimum water temperatures recorded by the UTR at 17m depth during 2006-2011 at Ponta Zavora, northern Delagoa Bight are indicated in Table 4.1. Note the records for 2006 and 2007 covered only 253 and 142 days respectively. The interannual variability revealed a minimum (~17.56°C) in October 2009 and a maximum (~28.70°C) in January 2011. The highest temperature amplitude (~10.2°C) was in 2009, whereas the lowest was in 2007 (~7.2°C), (Figure 4.13). Cool water events with periodicities of ~8-15 days were observed during 2006, 2008, 2009 and 2010, whereas they lasted 20-60 days during 2007 and 2010.

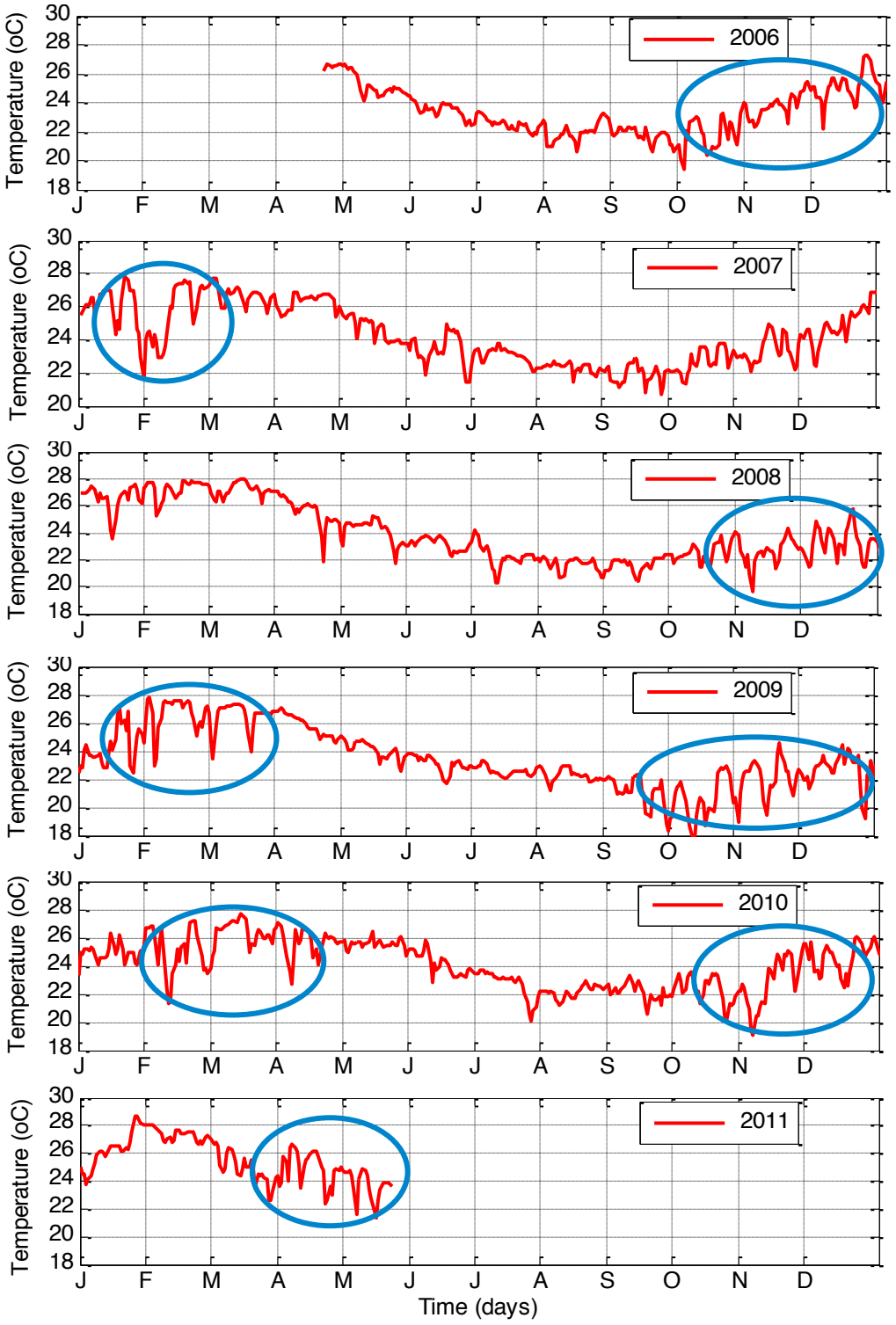

Figure 4.10: Time series of mean water temperature at 17m depth in Ponta Zavora (24.48°S, 35.24°E), northern Delagoa Bight (Figure 2.1), recorded from 23 April 2006 to 22 May 2011. Blue circles highlight cool water events (~2°C decrease).

Table 4. 1: Dates of the maximum and minimum temperatures recorded at 17m depth during 23 April 2006- 22 May 2011 at Ponta Zavora, northern Delagoa Bight. The records for 2006 and 2007 covered only 253 and 142 days respectively.

Year	Min (°C)	Date of Min	Max(°C)	Date of Max	Amplitude(°C)	Trend ($\mathbf{R^2}$)
2006	19.4	2 Oct	27.2	24 Dec	7.8	0.01
2007	20.7	30 Jan	27.9	24 Sep	6.2	0.33
2008	19.7	3 Nov	28.0	14 Mar	8.3	0.57
2009	17.6	9 Oct	27.9	2 Feb	10.3	0.51
2010	19.0	3 Nov	27.7	15 Mar	8.7	0.28
2011	21.4	15 May	28.7	25 Jan	7.3	0.40

The winds in the Delagoa Bight during 2006-2011 (not shown) blew predominantly towards the shore, although sporadic alongshore upwelling favourable winds (NE) were observed. Figure 4.14 shows snapshots of the winds that prevailed during the day before and on the day of the lowest temperatures in 2007, 2008, 2009 and 2010, the years with complete UTR records. According to these figures, the prevailing daily winds in the Delagoa Bight were from the NE (towards SW), the coastal upwelling favourable winds, with exceptions observed on the 24 September 2007 and 9 October 2009 (the latter was the day of the lowest temperature in the six year time series). The average wind speed in the whole bight ranged from ~7-11 $m.s^{-1}$ except for the 23 September 2007, when they registered relatively low speeds of ~2-6 $m.s^{-1}$. Furthermore, during September 2007, the wind speeds were higher in the northern Delagoa Bight than in the south.

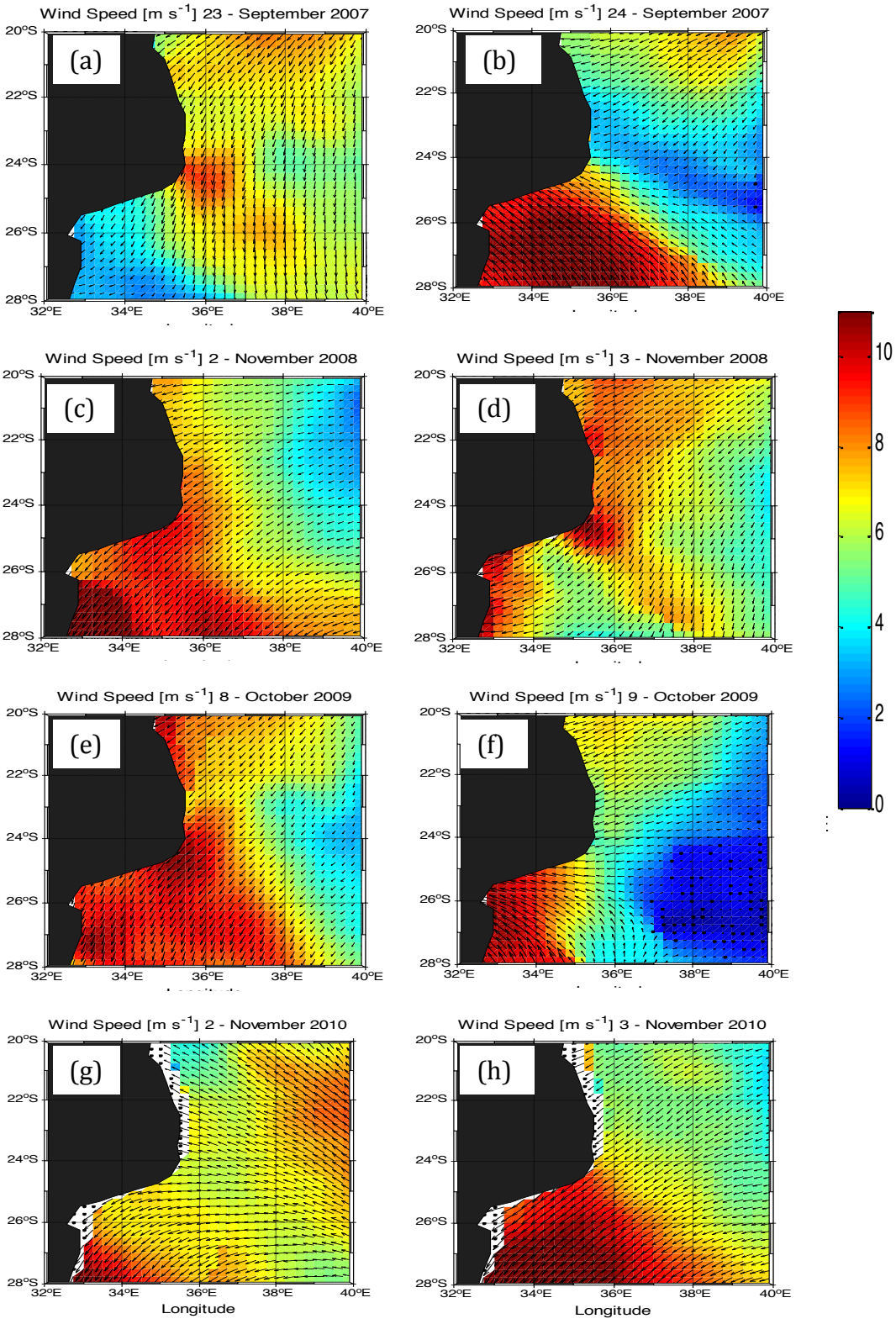

Figure 4.11: Snapshots of the daily winds observed a day before (left panel) and on the day(right panel) of the lowest temperatures at 17 m in Ponta Zavora (24.48° S, 35.24° E), northern Delagoa Bight during 2007-2010.

4.3.2. Cool water events at Ponta Zavora, northern Delagoa Bight

Wavelet analysis was performed in the time series of daily and daily anomalies of water temperature recorded at Ponta Zavora with the aim of extracting the dominant periodicities of variability. The power spectrum, Figure 4.15, of the de-meaned nor normalized time series of daily water temperature depicts a 95% statistically significant recurrent cycle of ~365 days (~12 months) periodicity.

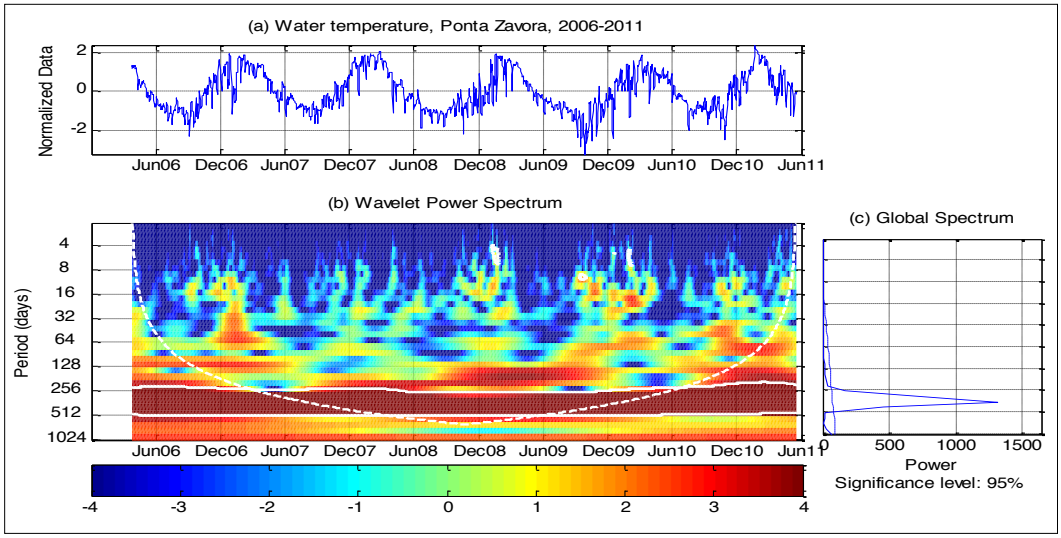

Figure 4.12: (Morlet) Wavelet analysis for water temperature (17 m) at Ponta Zavora (24.48° S, 35.24° E) from 2006 to 2011 showing statistically significant periods of about 365 days. (a) Wavelet power spectrum, (b) global wavelet spectrum with thick contours enclosing area of greater than 95% for a red-noise process. (Torrence and Compo, 1998).

The wavelet analysis on the de-meaned and normalized time series of daily water temperature is represented in Figure 4.16. The time series anomalies (Figure 16a) shows the cool water events recorded at 17 m. The wavelet power spectrum (Figure 16b) shows cool water events occurring every year from September (late winter) to April (early autumn). The global spectrum (Figure 4.16c) suggests that 95% statistically significant cool water events with duration of 3-15 days were frequent during 2006, 2008, 2009 and 2010. Relatively longer significant cool water events of ~20-60 days were observed during 2006 and 2010 (Figure 4.16).

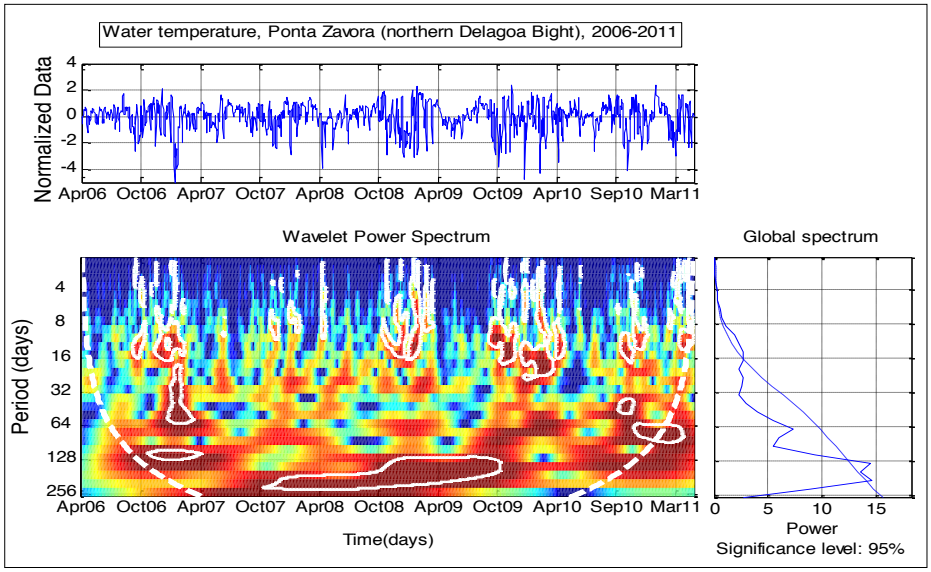

Figure 4.16:(Morlet) Wavelet analysis for water temperature time series from (17m depth) at Ponta Zavora (24.48^{o}S, 35.24^{o}E) from 2006 to 2011 showing statistically significant periods of cool water events of 8, 15, 30 and 50 days. (a) Wavelet power spectrum, (b) global wavelet spectrum with thick contours enclosing area of greater than 95% for a red-noise process. (Torrence and Compo, 1998).

From the wavelet power spectrum (Figure 4.16b) it was noted that the year 2009 was characterized by higher frequency of cool water events. In addition this year registered the highest interannual water temperature amplitude (~10.2^{o}C). For further purposes we chose the period 10th- October-30th December 2009 to further examine the cool coastal water events and the concurrent MODIS Aqua SST, the SSW and SLA (Figure 17). Dailly insitu water anomalies of ~4.0^{o}C were observed (Figure 17a) concurrent with winds blowing towards the shore with episodic NE winds (upwelling favourable winds), (Figure 17b). The MODIS Aqua weekly composite for Delagoa Bight suggests sea surface temperatures of ~ 21-23^{o}C and depicts a dipole like structure (Figure 17c) coherent with the weekly map of SLA for the period suggesting the prevalence of negative SLAs in the study region (Figure 4.17d).

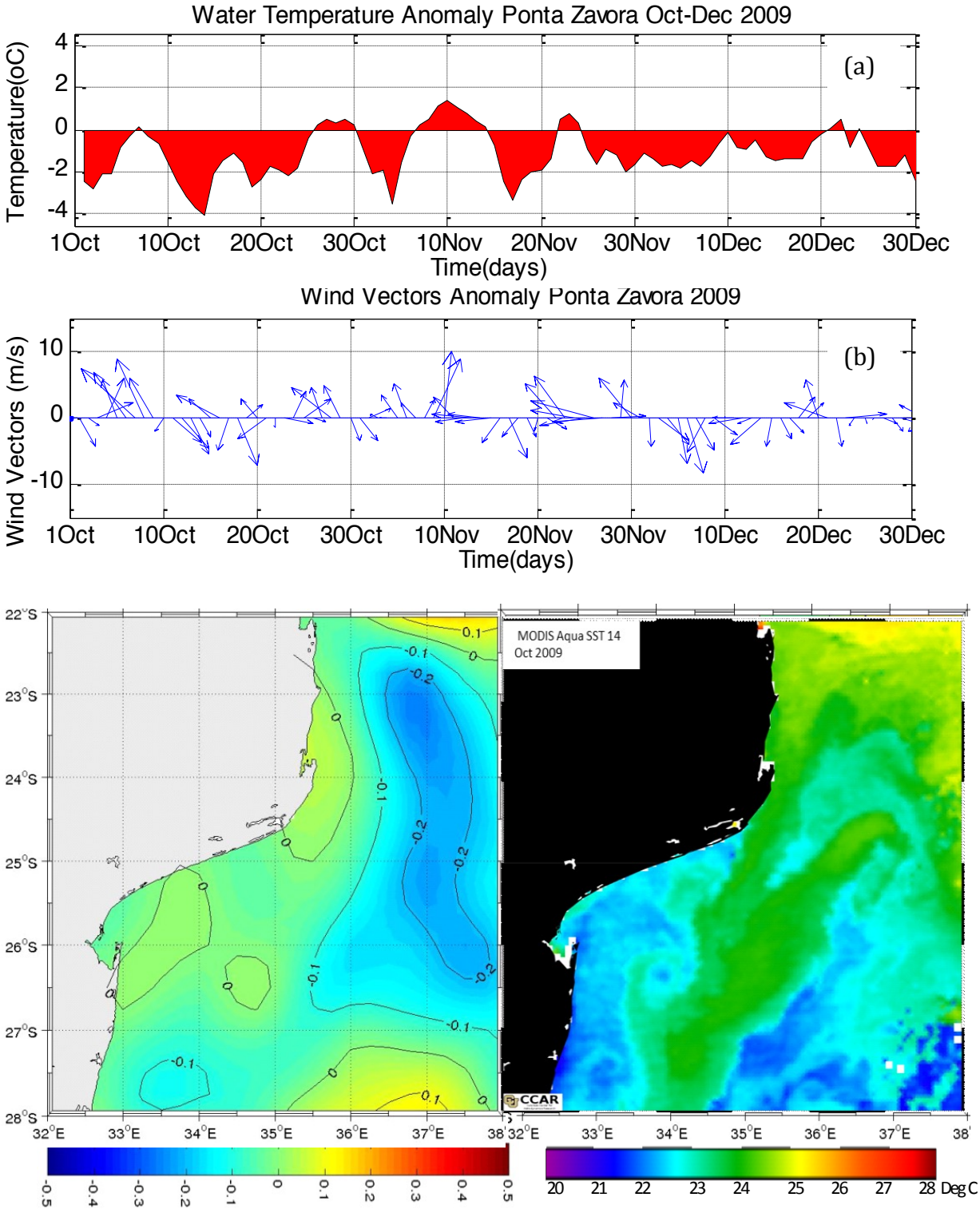

Figure 4.13: Anomalies of (a) water temperature at 17m, (b) wind vectors at Ponta Zavora (24.48°S, 35.24oE) during October –December 2009, (c) MODIS Aqua SST and (d) AVISO weekly SLA 14 October 2009 for the Delagoa Bight.

CHAPTER FIVE – DISCUSSION

Phytoplankton is one of the biological communities affected by the environmental change at the land-sea interface, therefore requiring continuous efforts for monitoring its dynamics, which is critical for understanding marine food webs and global climate (Srokosz, 2000; Winder and Cloern, 2010; Blondeau- Patissier et al., 2014). The majority of the existing research on the phytoplankton abundance (*Chl-a* concentration) and its interaction with the physical drivers for Delagoa Bight region results mainly from the use of short term datasets (*in-situ* and satellite) and from research designed for larger domains e.g. the Agulhas Current System and the Mozambique Channel (e.g. Quartly and Srokosz, 2004; Kai and Marsac, 2009, Roberts et al., 2014).

The research from these authors has advanced knowledge of the biophysical processes with major achievements from its application to the relevant disciplines, though further studies using finer spatial and temporal scales are required in order to increase the understanding of how the Delagoa Bight ecosystem functions. In this study, the seasonal and interannual variability of *Chl-a* concentration and its relationship with physical drivers (sea surface temperature (SST), sea surface winds (SSW) and sea surface height (SSH)) for Delagoa Bight averaged area (24-28^{o}S, 32-36^{o}E) have been addressed using 10years (2003-2012) of satellite monthly data. Further, the frequency and duration of cool water events (~2^{o}C decrease) in the northern Delagoa Bight have been assessed using 5-year (2006-2011) time series of *in situ* water temperature from a probe moored at 17 m at Ponta Zavora (24.48^{o}S and 35.24^{o}E*)*. A detailed discussion of the findings is presented in sections 5.1-5.3.

5.1. Seasonal variability of *Chl-a*, SST and SSW

The *Chl-a* concentration at the surface of the ocean generally responds to the seasonal cycle of solar radiation, which exerts a strong impact on the timing and intensity of vertical nutrient flux and vertical stability (Dandonneau et al., 2004). The 10-years seasonal climatology (Figure 4.1, Figure 4.2) shows the surface *Chl-a* increasing from June to September (late autumn-late winter) and decreasing from October to May (early spring-mid autumn), with the maximum in August and minimum in December. These results are

consistent with the findings from previous studies (Quartly and Srokosz, 2004; Barlow et al., 2008; Lamont et al., 2010; Sá et al., 2013). Quartly and Srokosz (2004) using SeaWiFS data describe a spring bloom with a maximum in July-August, caused by the seasonal increase in solar radiation and thermal stratification after winter mixing redistributes nutrients to surface waters (Quartly and Srokosz, 2003). Figure 4.2a shows the *Chl-a* seasonal cycle ranging from 0.14 $mg.m^{-3}$ (December 2009) to 0.39 $mg.m^{-3}$ (August 2003).

Chl-a concentration enhanced events (*Chl-a* blooms) with significant periodicities of 2-15 weeks (not shown) occur in Delagoa Bight throughout the year, with major peaks frequent in autumn-winter. Quartly and Srokosz (2004) and Sá et al. (2013) describe *Chl-a* concentrations for Delagoa Bight ranging from 0.09 to 1.6 $mg.m^{-3}$. The discrepancies between the *Chl-a* concentration range they describe and the results from this study may derive from the differences in the size of the study domain and the data extraction methodologies used in both studies. The spatial distribution of the surface *Chl-a (*Figure 4.1a) exhibits a non-homogeneous seasonal variability with an inshore-offshore gradient of enhanced *Chl-a* concentration (>0.5 $mg.m^{-3}$) along the coastal strip (shallower depths) and oligotrophic conditions of *Chl-a* concentration *(*~0.1 $mg.m^{-3}$) in the offshore waters. This pattern is in accordance with the general ocean production where higher phytoplankton biomass occurs in the coastal waters (Case 2 waters) associated with the increased load of nutrients and sediments brought by the continental runoff (Morel and Prieur, 1977; Yoder and Kennely, 2006).

Caution is taken in interpreting the *Chl-a* concentration estimated by satellite ocean colour sensors in the coastal waters (optically complex), as it can be overestimated due to the interference of non-pigment colour matters such as coloured dissolved organic matter (CDOM) (Yoder and Kennelly, 2006). High *Chl-a* concentration in the Delagoa Bight is associated with large volumes of nutrients brought downstream by the Limpopo River (Quartly and Srokosz 2004; Kyewalyanga et al., 2007). Distinct seasonal patterns of variability are apparent from the fields of SST and SSW, Figure 4.2 (b, c and d). The SST field (Figure 4.2b) exhibits a strong seasonal cycle of cooling from April to September (mid autumn-late winter) and warming from October to March (early spring- early autumn,) which seems to be associated with the seasonal cycle of solar heating (Lamont et al., 2010).

August is the coldest month (~22.4^{o}C) and February is the warmest (~27.4^{o}C), with the SST amplitude of ~5^{o}C, as seen in Figure 4.2b. A similar water temperature range is described by Lamont et al. (2010) for the upper-mixed layer (50-75m) as inferred from four hydrographic datasets collected during the ACEP cruises in May 2004, August 2004, April 2005 and April 2006.

Seasonal winds blowing towards the bight (onshore winds) prevailed during 2003-2012 as suggested by the climatological means, shown in Figure 4.2 (c and d). Similar results are described by Saetre and Da Silva (1982) and Lutjeharms (2006). The mean magnitude of the seasonal winds was weak (~3.0 m.s^{-1}) (Figure 4.2c and Figure, 4.2d). The seasonal variability did not depict the alongshore NE coastal upwelling favourable winds.

Coherence between the periods of increasing phytoplankton biomass *(Chl-a* concentration*)* and decreasing SSTs is suggested by the inverse seasonal cycles, (Figure 4.2a, Figure 4.2 b). Statistically highly significant anti-correlations ($p<0.001$) at time lag zero confirm the strong relationship between the *Chl-a* concentration and SST, with the year-to-year variability yielding correlations ranging from -0.68 in 2009, to -0.92 in 2004. Note that 2003 registered the maximum mean *Chl-a* concentration*,* whereas 2009 registered the minimum *Chl-a* concentration in the 10-year time series. The *Chl-a* and SST patterns contrast with the SSW patterns (Figure 4.2c, Figure 4.2d), lacking a clear seasonal cycle, which makes it difficult to assess their relationship with the *Chl-a* concentration. The timing of the *Chl-a* concentration maximum (August) seems to be triggered by the lowest seasonal temperatures and the onshore winds that prevailed during the study period. Figure 4.2 (a, c and d) suggests a time lag of about one month between the magnitude of the wind (zonal and meridional components) which registered the maximum in July preceding the seasonal maximum *Chl-a* concentration.

5.2. Interannual variability of *Chl-a*, SST and SSW

Delagoa Bight is one of the Mozambican shelf regions with enhanced *Chl-a* concentration (Quartly and Srokosz, 2004; Sa et al., 2013). Interannual variability of *Chl-a* concentration shows year-to-year shift in the timing and magnitude of the peaks (Figure 4.4a). The lowest *Chl-a* concentration (0.13 mg.m^{-3}) is observed in 2009 (December) and the highest (0.54

mg.m^{-3}) in 2003 (August). Figure 4.4.b shows that 2011 registered the lowest SST (21.7^{o}C) while 2006 registered the maximum (27.9^{o}C). The predominant winds are mainly blowing towards the shore with episodic coastal upwelling favourable winds of ~3.0 m.s^{-1} (Figure 4.4.c). The interannual variability of winds field (Figure 4.4c) exhibits a lack of seasonality, with the NE winds occurring sporadically, for example from May 2009– April 2012. Further examination of the NE winds shows a general lack of coherence with the *Chl-a* concentration. A possible explanation could be that the wind magnitude and the speed are not optimal to induce the upwelling process.

The timing of the maximum *Chl-a* concentration is consistent with the results from Quartly and Srokosz (2003) which describe a spring bloom with maximum biomass during July-August in the waters around the Agulhas Current System. The spring bloom is a canonical *Chl-a* concentration feature in the ocean and it is triggered by the increase in light and the enhanced water column stratification (Quartly and Srokosz, 2003). Wavelet analysis reveals significant periodicities in the *Chl-a* concentration variability interpreted as periods of phytoplankton growth which shows a recurrent seasonal cycle of ~12 months throughout the 10-years period (Figure 4.5). Similar to the *Chl-a* variability, there is a recurrent SST annual cycle (Figure 4.6) though the SST signal is weak during 2009 (Figure 4.6). It is worth to note that during the 10-years study period the year 2009 registered the lowest phytoplankton biomass and this was consistent with the decreasing cold anomalies that prevailed throughout the whole year (Figure 4.8a-b). The wind speed wavelet power spectrum present significant short periodicities at ~4 months band from 2003-2009 (Figure 4.7).

The time series of non- seasonal variations (anomalies) over the 10- years period (2003-2012), Figure 4.8 depict episodic events of coherence between the *Chl-a,* SST, SSW and SLA. Examples of the lack of coherency between the *Chl-a* and the SST are observed in 2006-2008 (Figure 4.8 a and Figure 4.8b), with both variables being simultaneously positive, whereas during 2008-2010 both are simultaneously negative, suggesting instability in the water column due to biophysical processes. A striking event of anomalous growth in the phytoplankton biomass is observed from July 2003-March 2004 (Figure

4.9a). This event is consistent with negative SST anomalies (Figure 4.9b), suggesting a vertical mixing due to physical mechanisms such as upwelling events, winds and mesoscale eddies which can uplift cold waters and thus increase *Chl-a* concentration (Kahru et al, 2010). The convergence process due to mesoscale cyclone eddies (negative SLA in the southern hemisphere) can uplift necessary cold and nutrient rich waters to the surface where the phytoplankton thrives, thus sustaining biomass growth (Roberts, 2014). Figure 4.10 suggests the prevalence of negative SLA in Delagoa Bight during the anomalous event relatively elevated *Chl-a* concentration. It is worth noting that altimetry data for regions near the land, as in the case of the Delagoa Bight region, is inaccurate. Upwelling favourable winds for Delagoa Bight are observed sporadically though they are not coherent with variation of the *Chl-a* concentration and the SST (Figure 11a-c).

Interannual variability suggest that 2005, 2007 and 2010 registered relatively higher SSTs above the average (Figure 4.8b). The warmest SST anomaly (0.78 ^{o}C) registered in 2005 was concurrent with a non- significant increase in the *Chl-a* concentration, Figure 4.8 (a and b). Episodic events of negative SST and positive *Chl-a* concentration anomalies are observed in Figure 4.8(a and b), e.g. during July 2003 - March 2004. The warmest SST anomalies observed in Delagoa Bight are consistent with the global air temperature records, wherewith 2005 being one of the two warmest years since 1850 (Pachauri, 2014). One of the major factor driving the interannual climate variability at the global scale is ENSO which can in turn affect the *Chl-a* variability (Murtugudde et al., 1999; Curie et al., 2013). Research to assess the impact of the climate indices in the SST and *Chl-a* concentration interannual variability in Delagoa Bight are still lacking.

5.3. Frequency and duration of cool water events in the northern Delagoa Bight

The uplift of the cold and nutrient rich waters from the subsurface to the euphotic zone, where light is mostly available, represents an important mechanism for the phytoplankton growth (Kahru et al., 2010). The phytoplankton abundance in Delagoa Bight is associated with an upwelling cell in the northern shore (Lutjeharms and Da Silva, 1988; Quartly and Srokosz, 2004; Lamont et al., 2010).

The occurrence of cool coastal water events of ~20-60 days periodicities occur in the northern Delagoa Bight at Ponta Zavora (24.48 ^{o}S- 35.24^{o} E) as suggested by y the analysis of daily water temperatures recorded at 17 m depth during the period 2006-2011. Cool coastal water events (Figure 4.13, Figure 16 and Figure 18a) occur mostly in summer and spring, with maximum amplitude of 6^{o}C. Further analysis of this daily data did not reveal the timing of such events to be regular, contrasting with the results from Malauene et al. (2014), who used 5-years of UTR data to investigate cool water events at Angoche (northern shelf of Mozambique) and reported regular events throughout their study period. This discrepancy could be due to the difference in the oceanographic processes acting in both sites. The investigation of the driving mechanisms of cool water events in Delagoa Bight was out of the scope of this research, though an exploratory approach, made by correlating the cool water events to physical variables, exhibited a modest significant correlation between the water temperature anomalies and the wind (meridional component and speed).

CHAPTER SIX – SUMMARY AND CONCLUSIONS

In this study we have analysed 10- years (2003-2012) of multi satellite monthly time series aimed at describing the seasonal and interannual variability of *Chlorophyll-a* concentration (*Chl-a*) and its relationship with sea surface temperature (SST), sea surface winds (SSW) and sea level anomalies (SLA) in the Delagoa Bight, averaged over the area (24-28^{o}S-32-36^{o}E). Further, we used ~5-years (2006-2011) of *in situ* daily water temperature dataset to describe the frequency and duration of cool coastal water events (~2^{o}C decrease) recorded at 17 m depth in the northern Delagoa Bight at Ponta Zavora (24.48 ^{o}S- 35.24^{o} E). From the area averaged study time series, we draw the following conclusions:

- The *Chl-a*, SST, SSW and SLA exhibited distinct patterns of variability. Strong seasonal structure was found in the area averaged *Chl a* (0.244 mg.m^{-3}) and SST.
- The *Chl-a* concentration increased from June through September (late autumn - late winter) and decreased from December to May (late spring - mid autumn). The lowest maximum in monthly *Chl- a* was in December (0.127 mg.m^{-3}) and the highest in August (0.541 mg.m^{-3}). Seasonal *Chl-a* enhanced events (increasing phytoplankton biomass) were observed in coherence with cooler SSTs.

- The SST fields exhibited a strong seasonal cycle of cooling from April to September (mid autumn-late winter) and warming from October to March (early spring- early autumn). The lowest maximum in monthly SST was in September (21.8^{o}C) and the maximum in February (27.9 ^{o}C), which seems to be associated to the seasonal solar radiation cycle.

- Onshore winds prevailed during the study period with episodic upwelling favorable (NE) winds. Cyclonic like structures were observed as suggested by the weak negative SLA (-0.5 to 0.5 cm). Relationships between the *Ch-a*, SSW and the SLA lack a general coherence. There was lack of coherence between the NE winds and the *Chl-a* concentration, one possibility could be the weak intensity of the NE winds (~3, 0 m.s^{-1}), therefore their inability to induce the upwelling process.

- Strong interannual modulation was observed in the *Chl a* and SST. The long term (2003-2012) mean *Chl-a* was ~0.24 ± 0.10 $mg.m^{-3}$ while the SST mean was ~24.8±1.92^{o}C.

- Interannual variability indicates the year 2009 with the lowest anomalies of *Chl-a* concentration (-0.13 $mg.m^{-3}$) besides the concurrent cooler waters as suggested by the persistent SST negative anomalies during the whole year. The year 2003 registered the highest *Chl-a* concentration anomaly (0.16 $mg.m^{-3}$) which were coherent with cool SSTs. The coldest SST anomaly (-1.19 ^{o}C) in the 10- years SST time series for Delagoa Bight averaged area was observed during 2012 while the warmest (0.78 ^{o}C) was in 2005.

- Wavelet analysis revealed a recurrent (~12-month) annual cycle of *Chl-a* and SST. For the SST time series the signal is present throughout the 10-years (2003-2012) while for the *Chl-a* it was absent during 2009, the year of persistent negative SST anomalies.

- The daily observations of temperature at 17 meters depth, from the northern Delagoa Bight at Ponta Zavora (24.48 ^{o}S- 35.24^{o} E) for the period 2006-2011 have confirmed a seasonal signal with amplitude of about 6.5^{o}C.

- Cool coastal water events were found mostly in summer and spring, with maximum amplitude of 6^{o}C. Further analysis of this daily data did not reveal the timing of such events to be regular.

This study shows that satellite data provide valuable information to characterize the seasonal and interannual variations of *Chl-a,* SST, SSW and SLA in the Delagoa Bight, which would be difficult to get by using *in situ* data. The results presented here should be interpreted with caution taking into account that remote sensing data have limitations, especially in the coastal shallow waters. Generally, the remote sensed *Chl-a* data for the Case 2 waters regions, such as the Delagoa Bight, is overestimated due to the influence of the suspended sediments and dissolved organic matter (Yoder and Kennely, 2009).

Besides this, satellite data provides information only for the topmost layer. Besides the inaccuracy of the SLA in the coastal shallow areas, the SST data can be affected by clouds and this has been reported to occur in the Mozambican Channel and adjacent waters (Malauene, 2014). Apart from these described limitations, this study provides information that can improve the understanding on the *Chl-a* concentration (phytoplankton biomass) variability and its relationship with the physical drivers in the Delagoa Bight ecosystem. Another implication of this study includes its use for the conception of the next studies for the Delagoa region. Further analysis to improve the understanding of the seasonal and interannual *Chl-a* variability is required and it should combine *in situ,* satellite and modelling data. Additional studies should also investigate the influence of the cyclonic eddy centered at 26^{o}S and 34^{o}E (Lutjeharms and Da Silva, 1988), upwelling, river discharge and the global climate indices (e.g. ENSO) impacts on the biological biomass in the Delagoa Bight.

BIBLIOGRAPHY

Barlow, R., Kyewalyanga, M., Sessions, H., Van den Berg, M., & Morris, T. (2008). Phytoplankton pigments, functional types, and absorption properties in the Delagoa and Natal Bights of the Agulhas ecosystem. Estuarine, Coastal and Shelf Science, 80(2), 201-211.

Berrick, S., Pham, L., Leptoukh, G., Liu,Z., Rui,H., Shen,S., Teng, W. And Zhu,T. (2004). Multi-sensor distributive online processing, visualization, and analysis system. Proceedings IGARSS 2004, Anchorage, AK Sep 15-24, III, 2030-2033.

Biastoch, A., & Krauss, W. (1999). The role of mesoscale eddies in the source regions of the Agulhas Current. Journal of Physical Oceanography, 29(9), 2303-2317.

Blondeau-Patissier, D., Gower, J. F., Dekker, A. G., Phinn, S. R., & Brando, V. E. (2014). A review of ocean color remote sensing methods and statistical techniques for the detection, mapping and analysis of phytoplankton blooms in coastal and open oceans. Progress in oceanography, 123, 123-144.

Brown, C. (Ed.). (2006). Marine and Coastal Ecosystems and Human Well-Being: Synthesis. United Nations Publications.

Chelton, D. B., Schlax, M. G., Samelson, R. M., & de Szoeke, R. A. (2007). Global observations of large oceanic eddies. Geophysical Research Letters, 34(15).

Cloern, J. E. (1996). Phytoplankton bloom dynamics in coastal ecosystems: a review with some general lessons from sustained investigation of San Francisco Bay, California. Reviews of Geophysics, 34(2), 127-168.

Currie, J. C., Lengaigne, M., Vialard, J., Kaplan, D. M., Aumont, O., Naqvi, S. W. A., & Maury, O. (2013). Indian Ocean dipole and El Niño/Southern Oscillation impacts on regional chlorophyll anomalies in the Indian Ocean. Biogeosciences, 10, 6677-6698.

Da Silva, A. J. (1982). Water masses and circulation of the Mozambique Channel.

Dandonneau, Y., Deschamps, P. Y., Nicolas, J. M., Loisel, H., Blanchot, J., Montel, Y., ... & Bécu, G. (2004). Seasonal and interannual variability of ocean color and composition of phytoplankton communities in the North Atlantic, equatorial Pacific and South Pacific. Deep Sea Research Part II: Topical Studies in Oceanography, 51(1), 303-318.

DiMarco, S. F., Chapman, P., Nowlin, W. D., Hacker, P., Donohue, K., Luther, M., ... & Toole, J. (2002). Volume transport and property distributions of the Mozambique Channel. Deep Sea Research Part II: Topical Studies in Oceanography, 49(7), 1481-1511.

Ducklow, H. W., Steinberg, D. K., & Buesseler, K. O. (2001). Upper ocean carbon export and the biological pump. Oceanography-Washington Dc-Oceanography Society-, 14(4), 50-58.

Gill, A. E., & Schumann, E. H. (1979). Topographically induced changes in the structure of an inertial coastal jet: application to the Agulhas Current. Journal of Physical Oceanography, 9(5), 975-991.

Gregg, W. W., Casey, N. W., & McClain, C. R. (2005). Recent trends in global ocean chlorophyll. Geophysical Research Letters, 32(3).

Halo, I. F. (2012). The Mozambique Channel eddies: Characteristics and mechanisms of formation.

Halo, I., Penven, P., Backeberg, B., Ansorge, I., Shillington, F., & Roman, R. (2014). Mesoscale eddy variability in the southern extension of the East Madagascar Current: Seasonal cycle, energy conversion terms, and eddy mean properties. Journal of Geophysical Research: Oceans, 119(10), 7324-7356.

Harlander, U., Ridderinkhof, H., Schouten, M. W., & De Ruijter, W. P. M. (2009). Long-term observations of transport, eddies, and Rossby waves in the Mozambique Channel. Journal of Geophysical Research: Oceans (1978–2012), 114(C2).

Helbling, E. W., & Villafane, V. E. (2007). Phytoplankton and primary production. Fisheries & Aquaculture, Encyclopedia of Life Support Systems (EOLSS), Eolss Publishers, Oxford, UK [http://www. eolss. net].

Hoguane, A. M. (2007). Perfil diagnóstico da zona costeira de Moçambique. Revista de gestão costeira integrada, 7(1), 69-82.

Huggett, J. A. (2014). Mesoscale distribution and community composition of zooplankton in the Mozambique Channel. Deep Sea Research Part II: Topical Studies in Oceanography, 100, 119-135.

IMR, 1978. Cruise report no. 3 of RV' Dr. Fridtjof Nansen, January-March 1978. Joint NORAD/MOCAMBIQUE/FAO Project to investigate the fish resources off the Coast of Mozambique. Bergen, Norway.

Jose, Y. S., Aumont, O., Machu, E., Penven, P., Moloney, C. L., & Maury, O. (2014). Influence of mesoscale eddies on biological production in the Mozambique Channel: Several contrasted examples from a coupled ocean-biogeochemistry model. Deep Sea Research Part II: Topical Studies in Oceanography, 100, 79-93.

Kahru, M., Gille, S. T., Murtugudde, R., Strutton, P. G., Manzano-Sarabia, M., Wang, H., & Mitchell, B. G. (2010). Global correlations between winds and ocean chlorophyll. Journal of Geophysical Research: Oceans (1978–2012),115(C12).

Kai, E. T., & Marsac, F. (2010). Influence of mesoscale eddies on spatial structuring of top predators' communities in the Mozambique Channel. Progress in Oceanography, 86(1), 214-223.

Kirk, J. T. (1994). Light and photosynthesis in aquatic ecosystems. Cambridge university press.

Kletou, D., & Hall-Spencer, J. M. Threats to ultraoligotrophic marine ecosystem

Kyewalyanga, M. S., Naik, R., Hegde, S., Raman, M., Barlow, R., & Roberts, M. (2007). Phytoplankton biomass and primary production in Delagoa Bight Mozambique: Application of remote sensing. Estuarine, Coastal and Shelf Science, 74(3), 429-436.

Lalli, C. M., & Parsons, T. R. (1997). Biological oceanography: an introduction. Oceanographic Literature Review, 11(44), 1297.

Lamont, T., Roberts, M. J., Barlow, R. G., Morris, T., & van den Berg, M. A. (2010). Circulation patterns in the Delagoa Bight, Mozambique, and the influence of deep ocean eddies. African Journal of Marine Science, 32(3), 553-562.

Lau, K. M., & Weng, H. (1995). Climate signal detection using wavelet transform: How to make a time series sing. Bulletin of the American Meteorological Society, 76(12), 2391-2402.

Lutjeharms, J. R. (2006). The Agulhas Current.

Lutjeharms, J. R. E., & Da Silva, A. J. (1988). The Delagoa Bight Eddy. Deep Sea Research Part A. Oceanographic Research Papers, 35(4), 619-634.

Lutjeharms, J. R. E., & Da Silva, A. J. (1988). The Delagoa Bight eddy. Deep Sea Research Part A. Oceanographic Research Papers, 35(4), 619-634.

Malauene, B. S., Shillington, F. A., Roberts, M. J., & Moloney, C. L. (2014). Cool, elevated chlorophyll-a waters off northern Mozambique. Deep Sea Research Part II: Topical Studies in Oceanography, 100, 68-78.

McGillicuddy Jr., D.J., Robinson, A.R., Siegel, D.A., Jannasch, H.W., Johnson, R., Dickey, T.D., McNeil, J., Michaels, A.F., Knap, A.H., 1998. Influence of mesoscale eddies on new production in the Sargasso Sea. Nature 394, 263–265.

Morel, A., & Prieur, L. (1977). Analysis of variations in ocean color1. Limnology and oceanography, 22(4), 709-722.

Murtugudde, R. G., Signorini, S.R., . Christian, J.R., Busalacchi, A. J., McClain, C., R. and Picaut, J., (1999). Ocean colour variability of the tropical Indo-Pacific basin observed by SeaWiFS during 1997-1998. J. Geophy. Res. 104, C8, 18,351-18,366

O'Reilly, J. E., Maritorena, S., Siegel, D. A., O'Brien, M. C., Toole, D., Mitchell, B. G., ... & Culver, M. (2000). Ocean color chlorophyll a algorithms for SeaWiFS, OC2, and OC4: Version 4. SeaWiFS postlaunch calibration and validation analyses, Part, 3, 9-23.

Pachauri, R. K., Allen, M. R., Barros, V. R., Broome, J., Cramer, W., Christ, R., ... & van Vuuren, D. (2014). Climate Change 2014: Synthesis Report. Contribution of Working Groups I, II and III to the Fifth Assessment Report of the Intergovernmental Panel on Climate Change.

Platt, T. (2008). Why Ocean Colour?: The Societal Benefits of Ocean-colour Technology (No. 7). International Ocean-Colour Coordinating Group.

Quartly, G. D., & Srokosz, M. A. (2004). Eddies in the southern Mozambique Channel. Deep Sea Research Part II: Topical Studies in Oceanography, 51(1), 69-83.

Quartly, G. D., & Srokosz, M. A. (2003). Satellite observations of the Agulhas Current system. Philosophical Transactions of the Royal Society of London A: Mathematical, Physical and Engineering Sciences, 361(1802), 51-56.

Ridderinkhof, H., & De Ruijter, W. P. M. (2003). Moored current observations in the Mozambique Channel. Deep Sea Research Part II: Topical Studies in Oceanography, 50(12), 1933-1955.

Roberts, M. J., Ternon, J. F., & Morris, T. (2014). Interaction of dipole eddies with the western continental slope of the Mozambique Channel. Deep Sea Research Part II: Topical Studies in Oceanography, 100, 54-67.

Sá, C., Leal, M. C., Silva, A., Nordez, S., André, E., Paula, J., & Brotas, V. (2013). Variation of phytoplankton assemblages along the Mozambique coast as revealed by HPLC and microscopy. Journal of Sea Research, 79, 1-11.

Saetre, R., & da Silva, A. J. (1982). Water masses and circulation of the Mozambique Channel.

Schouten, M. W., de Ruijter, W. P., van Leeuwen, P. J., & Ridderinkhof, H. (2003). Eddies and variability in the Mozambique Channel. Deep Sea Research Part II: Topical Studies in Oceanography, 50(12), 1987-2003.

Srokosz, M. A. (2000). Biological oceanography by remote sensing. Encyclopedia of Analytical Chemistry.

Thomson, R. E., & Emery, W. J. (2014). Data analysis methods in physical oceanography. Newnes.

Torrence, C., & Compo, G. P. (1998). A practical guide to wavelet analysis. Bulletin of the American Meteorological society, 79(1), 61-78.

Van der Werf, P. M., Van Leeuwen, P. J., Ridderinkhof, H., & De Ruijter, W. P. M. (2010). Comparison between observations and models of the Mozambique Channel transport: Seasonal cycle and eddy frequencies. Journal of Geophysical Research: Oceans (1978–2012), 115(C2).

Vantrepotte, V., & Mélin, F. (2009). Temporal variability of 10-year global SeaWiFS time-series of phytoplankton chlorophyll a concentration. ICES Journal of Marine Science: Journal du Conseil, fsp107.

Wernand, M. R., van der Woerd, H. J., & Gieskes, W. W. (2013). Trends in ocean colour and chlorophyll concentration from 1889 to 2000, worldwide.

Winder, M., & Cloern, J. E. (2010). The annual cycles of phytoplankton biomass. Philosophical Transactions of the Royal Society B: Biological Sciences, 365(1555), 3215-3226.

Zhang, H. M., Reynolds, R. W., & Bates, J. J. (2006, January). Blended and gridded high resolution global sea surface wind speed and climatology from multiple satellites: 1987–present. In American Meteorological Society 2006 Annual Meeting, Paper P (Vol. 2).